

Ecophenotypic plasticity versus evolutionary trends—morphological variability in Upper Jurassic bivalve shells from Portugal

SIMON SCHNEIDER, FRANZ T. FÜRSICH, TANJA SCHULZ-MIRBACH, and WINFRIED WERNER



Schneider, S., Fürsich, F.T., Schulz-Mirbach, T., and Werner, W. 2010. Ecophenotypic plasticity versus evolutionary trends—morphological variability in Upper Jurassic bivalve shells from Portugal. *Acta Palaeontologica Polonica* 55 (4): 701–732.

Upper Jurassic marginal marine strata of the Lusitanian Basin (central Portugal) yield a rich benthic macrofauna from which three bivalve target taxa, i.e., *Arcomytilus*, *Isognomon*, and *Eomiodon*, were chosen for morphometric studies, because of their abundance both in space and time and their variability in shell shape. The shells have been analysed with regard to outline shape (Fourier shape analysis), dimensions, ornamentation (*Arcomytilus*) and ligament arrangement (*Isognomon*). Additionally, data on co-occurring fauna and palaeotemperatures calculated from $\delta^{18}\text{O}$ values have been recorded. The results of the morphometric analyses have been interpreted with regard to phylogeny and palaeoecology. In all target taxa, a distinct, rapid size increase at around the Early/Late Kimmeridgian boundary is evident. Potential causes for this process are discussed, and an increase in food availability is regarded the most likely scenario. In *Isognomon rugosus*, a distinct change in resiliifer arrangement co-occurs with size increase, resulting in the evolution of an endemic species in the Lusitanian Basin, for which the name *Isognomon lusitanicus* is re-established. Like in several extant Mytilidae, morphological species characterisation in *Arcomytilus* turns out unsatisfactory, due to high intra-specific variability. However, *Arcomytilus morrisii* is still regarded as a valid species that evolved in the Lusitanian Basin. Despite high shape variability, *Eomiodon securiformis* is also considered to be a clearly distinguished species. For all target taxa morphologic variability is discussed with regard to environment, and variation between populations is delineated. The data suggest a weak correlation of facies and shell shape in *Arcomytilus*, while *Isognomon lusitanicus* seems to develop local varieties in different subbasins. Finally, the great morphologic plasticity of bivalves from rather distinct systematic entities is shown to result from different causes, thus demonstrating that careful studies of the involved species are a prerequisite to draw correct palaeoecological conclusions.

Key words: Bivalvia, morphometry, Fourier shape analysis, size increase, ecophenotypy, Late Jurassic, Portugal.

Simon Schneider [s.schneider@lrz.uni-muenchen.de] and Winfried Werner [w.werner@lrz.uni-muenchen.de], Bayerische Staatssammlung für Paläontologie und Geologie and GeoBioCenter^{LMU}, Richard-Wagner-Str. 10, D-80333 Munich, Germany;

Franz T. Fürsich [franz.fuersich@gzn.uni-erlangen.de], GeoZentrum Nordbayern, Fachgruppe PaläoUmwelt, Friedrich-Alexander Universität Erlangen-Nürnberg, Loewenichstr. 28, D-91054 Erlangen, Germany;

Tanja Schulz-Mirbach [t.schulz-mirbach@lrz.uni-muenchen.de], Department für Geo- und Umweltwissenschaften, Paläontologie & Geobiologie, Ludwig-Maximilians-Universität München, Richard-Wagner-Str. 10, D-80333 Munich, Germany.

Received 26 May 2009, accepted 29 April 2010, available online 4 May 2010.

Introduction

Morphological species concepts represent the key to palaeontological systematics and are also among the most debated subjects in systematic biology (e.g., Stanley 1979; Willmann 1985). With increasing knowledge of ecophenotypic plasticity, established species concepts frequently have to be verified or modified, commonly in light of morphometric description of biological form (in bivalves: e.g., Roopnarine and Vermeij 2000; Anderson and Roopnarine 2005; Tang and Pantel 2005; Rufino et al. 2006; Roopnarine et al. 2008). Most bivalves are ideal subjects for studying the relationship

between morphology and ecology, as shape and growth of most bivalve shells are directly controlled by habitat-specific factors, such as substrate, space, temperature, salinity, nutrition, or competition, due to the more or less stationary epibenthic life style of these animals (Stanley 1970). Turning the tables, fossil bivalve shells directly record palaeoecological information that may be extracted by applying morphological and/or geochemical analyses, and therefore represent excellent tools for palaeoenvironmental studies.

In Jurassic bivalves, research on evolutionary processes and their relationships to palaeoecological factors is still in its infancy. With few exceptions (e.g., the profuse literature

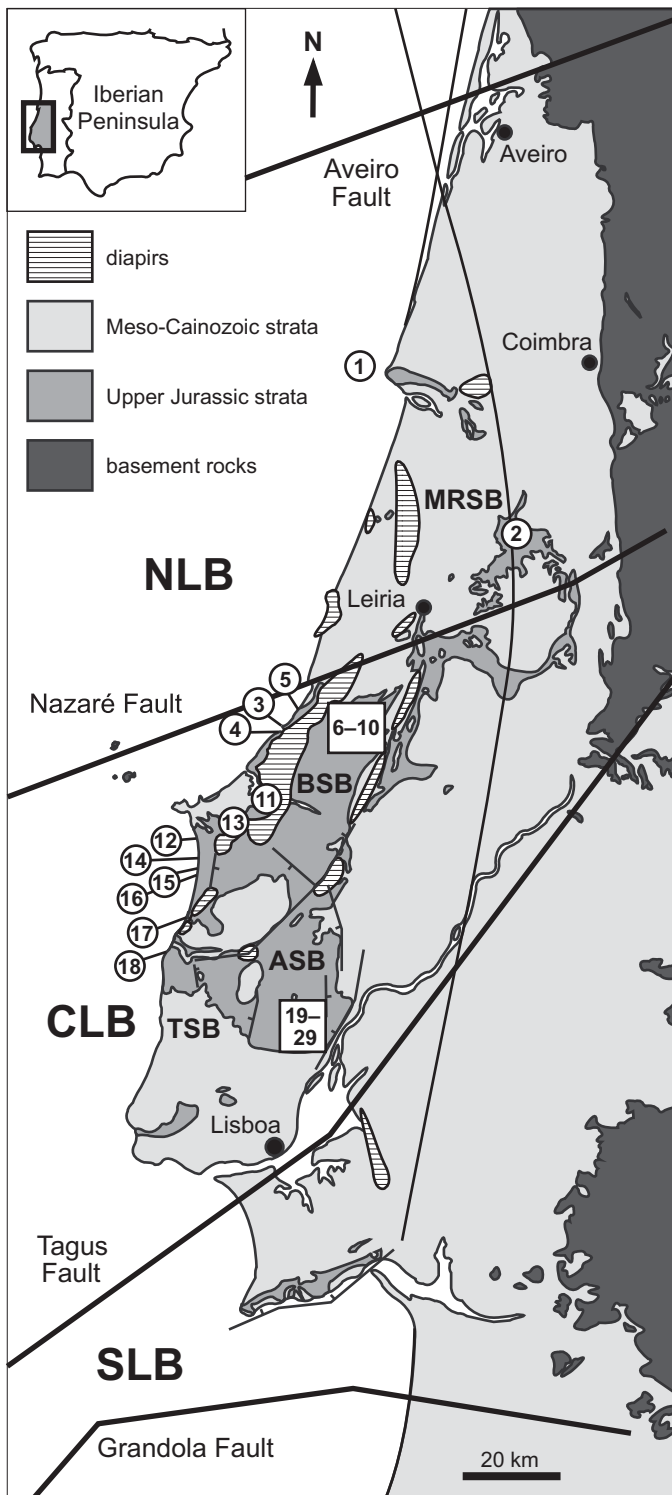


Fig. 1. Geographic and geological overview of the Lusitanian Basin. The numbering of localities refers to Table 1, second column.

on *Gryphaea*; see Hallam 1968; Johnson 1994; Nori and Lathuilière 2003, and references therein), previous studies mainly focused on the qualitative and quantitative nature of such processes but largely failed to explain the potential causes (e.g., Hallam 1975, 1998; Johnson 1984).

Several taxa of Upper Jurassic bivalves from the Lusitanian Basin (central Portugal; Fig. 1) occur during a comparatively long time-span (Late Oxfordian–Late Tithonian; Fig. 2) and in high abundance, and thus represent ideal objects for a comprehensive morphometric analysis. During the Late Jurassic, the Lusitanian Basin was a semi-enclosed basin, comprising to a large extent marginal marine, brackish water, and freshwater habitats. Many of the siliciclastic and carbonate strata deposited during this period are characterised by a rich and high-quality fossil record. Commonly, the macrobenthic assemblages preserved in these sediments are dominated by bivalves, which provide an adequate sample density and sample quantity amenable to statistical analysis of the target taxa for this study, i.e., the genera *Arcomytilus*, *Isognomon*, and *Eomiodon* (Figs. 3–5). Generally, these three bivalve taxa thrived in low-diversity/high-frequency associations in brackish-water habitats, but all of them are also found in associations attributed to have lived under normal marine conditions (Fürsich and Werner 1986). As a typical member of the family Mytilidae, *Arcomytilus* is characterised by a dyso-dont hinge and mytiliform shell ornamented with numerous radial ribs. It lived byssally attached to hard substrate or (bio-)clasts, as either an epibenthic or semi-infaunal edgewise recliner sensu Seilacher (1984) when settling on soft bottoms. A similar semi-infaunal, edgewise reclining life style is reported for the members of *Isognomon* that are included in this study (Fürsich 1980). The type genus of the Isognomonidae encompasses species of rather disparate shapes which are characterised by an evenly-spaced multi-vincular ligament and the absence of hinge teeth. Members of the genus *Eomiodon* (family Neomiodontidae) generally have a simple veneroid shell-shape, occasionally ornamented with a few sharp-crested commarginal ribs, and a marked inset escutcheon, and lived as shallow-infaunal suspension-feeders. The representatives of *Eomiodon* from Portugal are among the largest ones of this genus.

Research on Upper Jurassic bivalves from Portugal started in 1850, when Sharpe described and figured selected taxa as part of a study on the geology of the central Lusitanian Basin (Sharpe 1850). These reports were followed by a monographic account of the Jurassic bivalves by Choffat (1885, 1893). After a long phase, research on these organisms was revived, resulting in a set of publications mainly on their taxonomy, palaeoecology, and taphonomy (Fürsich and Schmidt-Kittler 1980; Fürsich 1981a, b; Fürsich and Werner 1984, 1985, 1986, 1988, 1989a, b, 1991; Freneix and Quesne 1985; Werner 1986; Schneider and Werner 2007). In the course of these studies, the supposedly endemic nature of several species was recognised and preliminary observations on the variability of species and potential phylogenies were made.

The present case study on three bivalve genera (*Arcomytilus*, *Isognomon*, and *Eomiodon*) from the Upper Jurassic of the Lusitanian Basin substantiates these observations by analysing the morphological variation of shells in their palaeoecological and evolutionary context. The signifi-

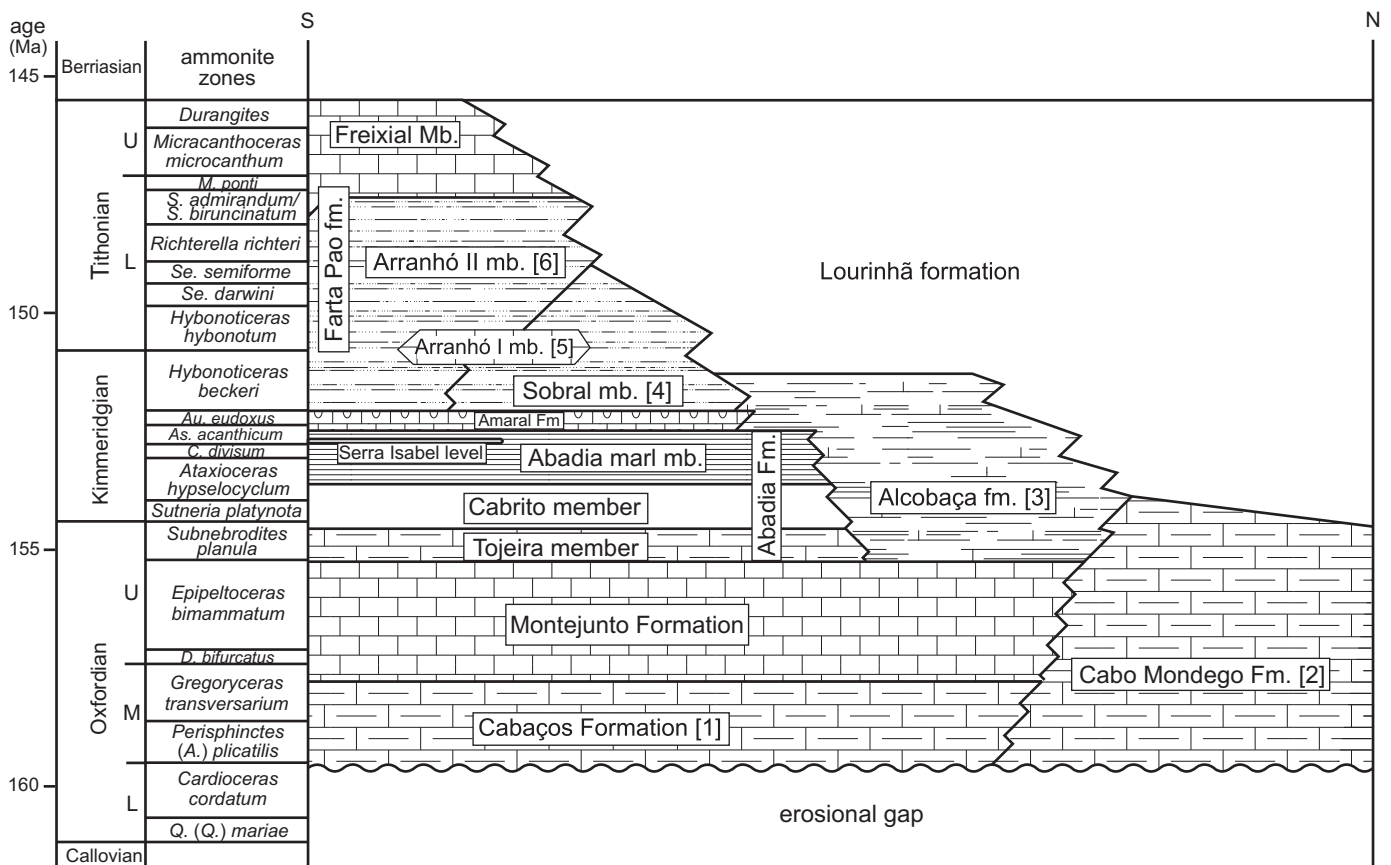


Fig. 2. Lithostratigraphy of the Upper Jurassic rock suite in the Lusitanian Basin. Modified from Schneider et al. (2009). All units discussed herein are numbered in squared brackets. Formations and members that are not yet formally established are written in lower case letters. Abbreviations: A., *Arisphinctes*; As., *Aspidoceras*; Au., *Aulacostephanus*; C., *Crussoliceras*; D., *Dichotomoceras*; Fm., formation; M., *Micracanthoceras*; Mb., member; Q., *Quenstedtoceras*; S., *Simoceras*; Se., *Semiformiceras*.

cance of the study lies both in the extraordinarily large data set (~1400 individuals) and in the temporal and spatial sampling density, which are prerequisites in order to unravel morphological changes with time or between different habitats. However, our aim is not only to identify these changes qualitatively and quantitatively in order to be able to evaluate potential endemism of species, but also to find palaeobiological explanations for these processes. In order to achieve these goals, a variety of techniques including oxygen isotope analysis, linear measurements and counting methods, but predominantly Fourier shape analysis, are applied, and the results are combined with palaeoecological information from the fossil assemblages.

Institutional abbreviations.—BSPG, Bayerische Staatssammlung für Paläontologie und Geologie, Munich, Germany; IGM, GML, Muséu Geológico, Instituto Geológico e Mineiro, Lisbon, Portugal; MNHN, Muséum National d'Histoire Naturelle, Paris, France.

Other abbreviations.—CLB, central Lusitanian Basin; FFT, Fast Fourier Transformation; NLB, northern Lusitanian Basin; PCA, Principal Component Analysis; SLB, southern Lusitanian Basin; VCV, variance-covariance.

Geographic and geological overview

The Lusitanian Basin stretches along the western margin of central Portugal (Fig. 1). Including the shelf areas, it extends for approximately 300 km in length and 180 km in width (Montenat et al. 1988). Onshore, the Lusitanian Basin reaches from Aveiro in the north to the Serra d'Arrabida south of the Tagus River. To the east it is bordered by basement rocks of the Iberian Meseta. To the west, crystalline remnants of the former basin margin are exposed on the Berlenga Horst (Carvalho et al. 2005).

Genetically, the Lusitanian Basin is a syn-rift basin related to the opening of the Atlantic Ocean, and is situated at a passive continental margin (e.g., Wilson 1975; Wilson et al. 1989; Alves et al. 2002). The basin started to open in the Late Triassic and is partitioned into a northern (NLB), central (CLB), and southern (SLB) sector by two reactivated Variscan major faults, i.e., the Nazaré and Tagus faults. Triggered by rapid rifting during the Late Jurassic, the basin began to differentiate into several subbasins, which developed as a result of diapirism that led to the formation of salt diapirs pre-

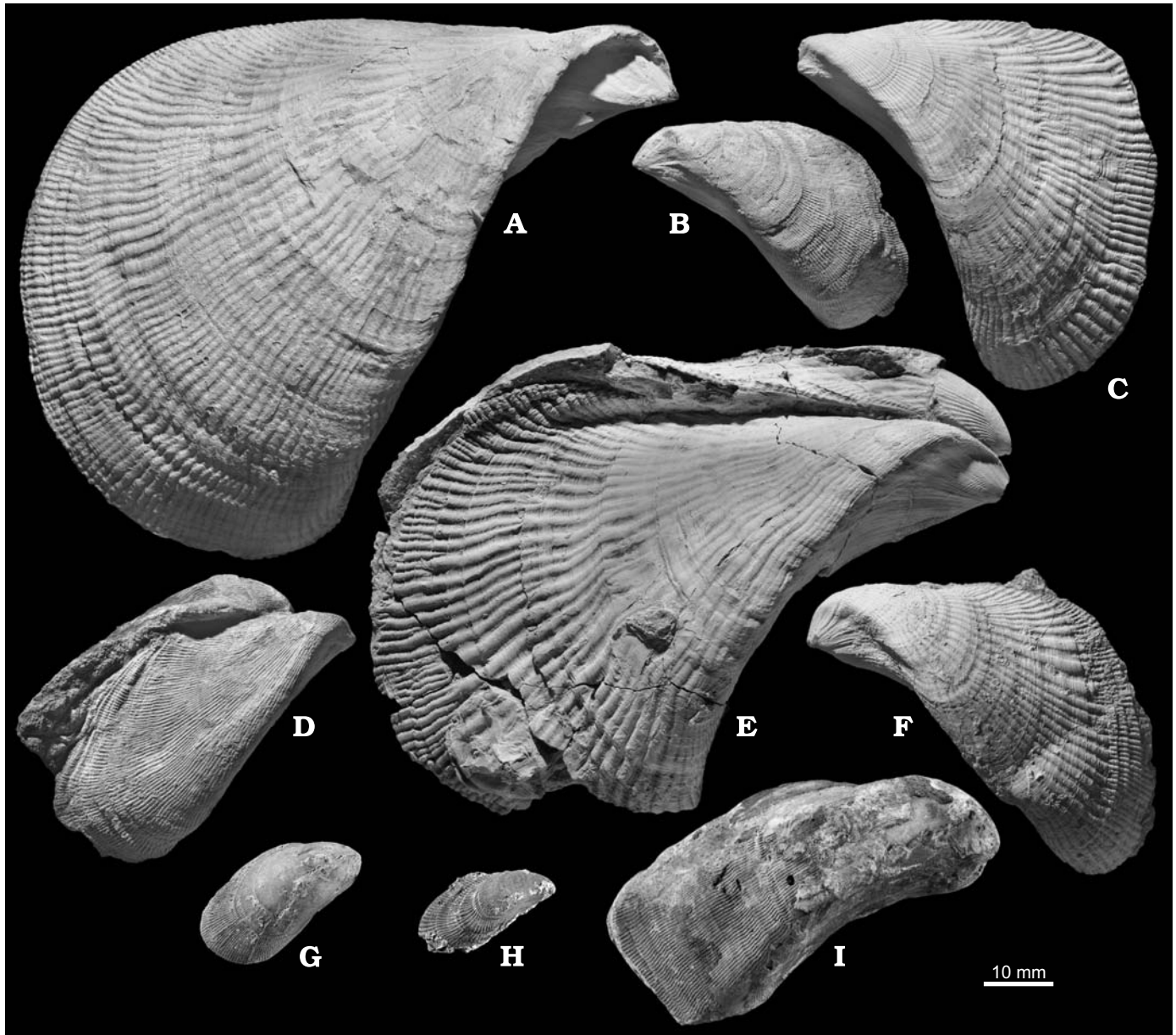


Fig. 3. Specimens of mytilid bivalve *Arcomytilus* from the Middle and Upper Jurassic of Portugal and France. **A–F.** *Arcomytilus morrisii* (Sharpe, 1850). **A.** Large articulated specimen with pointed umbones and slightly imprinted anterior part. Arranhó II member, earliest Tithonian, Serra de Alrota. GML 25900. **B.** Small adult specimen, left valve with fine ribbing pattern and relatively straight anterior margin. Alcobaça formation, Late Kimmeridgian, Consolação. GML 25901. **C.** Young adult specimen, left valve with coarse ribbing pattern and large, elevated disc. Arranhó II member, Early Tithonian, Santa Cruz. GML 25902. **D.** Small adult, articulated specimen. Alcobaça formation, Early Kimmeridgian, Salir do Porto. GML 25903. **E.** Large articulated specimen with extremely triangular outline and wide-spaced, strong ribs. Arranhó II member, Early Tithonian, Lameiro das Antas. GML 25904. **F.** Adult specimen, left valve with bi- and trifurcation and simultaneous insertion of ribs. Arranhó II member, Early Tithonian, Santa Cruz. GML 25905. **G.** *Arcomytilus asper*. Right valve. Late Bathonian, Luc-sur-Mer, Calvados, France. MNHN J 08224. **H.** *Arcomytilus bathonicus*. Right valve. Late Bathonian, Luc-sur-Mer, Calvados, France. MNHN, coll. Deshayes 1876-8. **I.** *Arcomytilus pectinatus*. Right valve. “Corallien”, La Rochelle, Charente-Maritime, France. MNHN, coll. d’Orbigny 4247.

dominantly along lineaments of Variscan origin (Alves et al. 2002, 2006; Carvalho et al. 2005).

Today, the Lusitanian Basin is filled with sediments of Late Triassic to Pleistocene age. The Upper Jurassic portion of this infill is up to 2700 m thick and forms a single mega-sequence (Alves et al. 2002). Following a phase of erosion, Upper Jurassic sedimentation started during the late Early/Middle Oxfordian. Consequently, Oxfordian deposits usu-

ally overlie Middle Jurassic rocks unconformably (Fig. 2). Progradation of sedimentary infill was directed towards the South because of a general dip of the basin axis from NNE to SSW, resulting in lithostratigraphic units that are diachronous at a large scale. A general update of the lithostratigraphy and a set of numerical ages for several of the strata have recently been presented by Schneider et al. (2009).

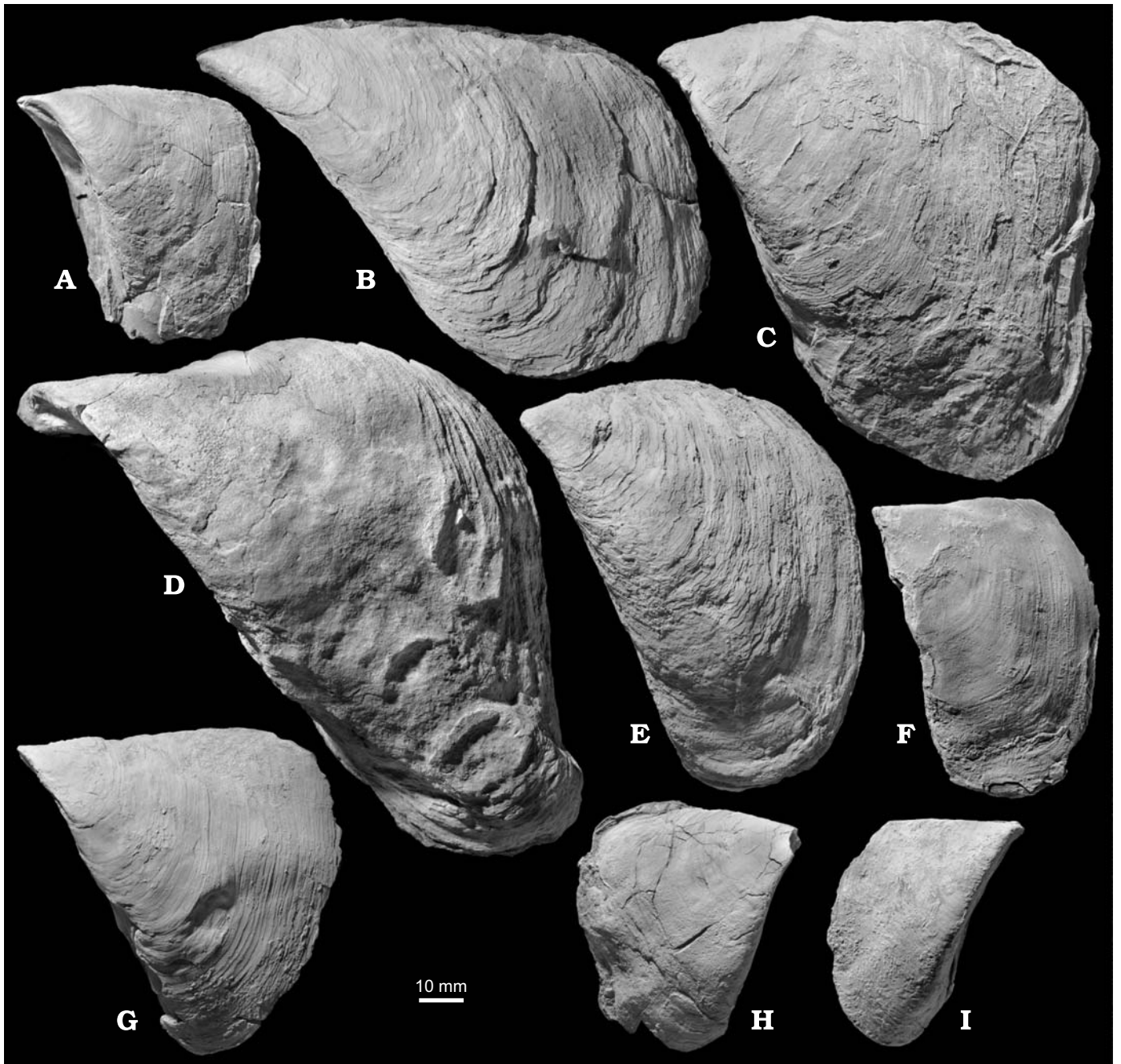


Fig. 4. Specimens of isognomonid bivalve *Isognomon* from the Upper Jurassic of Portugal. **A, F, H.** *Isognomon rugosus* (Münster in Goldfuss, 1835). **B–E, G, I.** *Isognomon lusitanicus* (Sharpe, 1850). **A.** Adult articulated specimen. Alcobaça formation, Early Kimmeridgian, Fonte Santa. GML 25906. **B.** Articulated specimen with pointed umbones. Alcobaça formation, Late Kimmeridgian, Consolação. GML 25907. **C.** Adult left valve. Arranhó II member, Early Tithonian, Santa Cruz. GML 25908. **D.** Strongly inflated articulated specimen with incurved umbones and slender, curved disc. Arranhó II member, Early Tithonian, S Rio Sizandro. GML 25909. **E.** Articulated, slender specimen with straight anterior margin and short umbones. Alcobaça formation, Late Kimmeridgian, Consolação. GML 25910. **F.** Partial mould with partially preserved calcitic outer shell layer. Alcobaça formation, Early Kimmeridgian, Salir do Porto. GML 25911. **G.** Triangular left valve. Arranhó II member, Early Tithonian, Santa Cruz. GML 25912. **H.** Articulated triangular specimen. Alcobaça formation, Early Kimmeridgian, Fonte Santa. GML 25913. **I.** Juvenile articulated, elongated, slender specimen, Sobral member, latest Kimmeridgian–earliest Tithonian, Chão da Cruz. GML 25914.

Material

The fossils for this study are derived from the Monte Real, Bombarral, Arruda, and Lower Tagus subbasins, and from a number of localities along the Atlantic coast (Fig. 1). Most

specimens were collected by the authors mainly during two field campaigns in 2005 and 2006. Most of the samples are derived from rocks exposed in road-cuts, quarries, and along the coastline. Several of the respective layers were analysed with regard to taphonomy and the time span and mode of

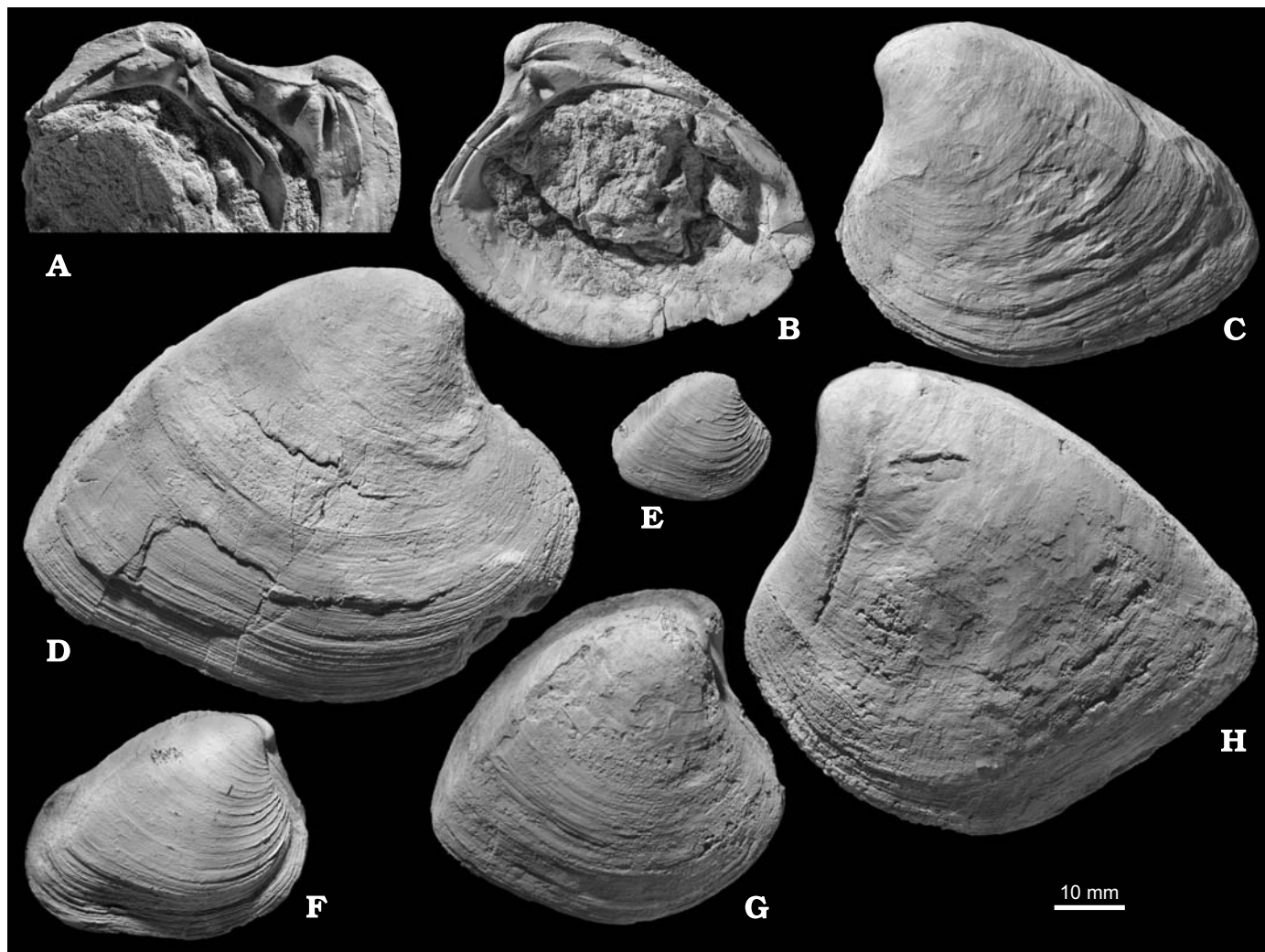


Fig. 5. Specimens of neomiodontid bivalve *Eomiodon securiformis* (Sharpe, 1850) from the Upper Jurassic of Portugal. A–C. Sobral member, Late Kimmeridgian, E Arranhó. A. Hinge plates of left and right valve. GML 25915. B. Interior of right valve, showing hinge arrangement and parts of the muscle scars. GML 25916. C. Left valve view of articulated specimen. GML 25917. D. Articulated, strongly elongated, gerontic specimen. Sobral member, Late Kimmeridgian, Santa Cruz. GML 25918. E. Small articulated specimen with clearly visible commarginal lamellae. Alcobaça formation, Early Kimmeridgian, Vestiaria. GML 25919. F. Articulated gerontic specimen with ventrally elongated shell. Alcobaça formation, Early Kimmeridgian, Salgados. GML 25920. G. Short, rounded, articulated specimen. Sobral member, Late Kimmeridgian, E Arranhó. GML 25921. H. Large, high, and short specimen. Sobral member, Late Kimmeridgian, Porto das Barcas. GML 25922.

their formation in a previous study (Fürsich et al. 2009). Other specimens were picked from weathered surfaces and ploughed fields, if the samples could be addressed to distinct horizons based on facies, faunal composition, and comparison with immediately adjacent exposures. In several cases, fossiliferous layers less than 20 cm thick could be traced this way across fields or vineyards. Additional material from the Choffat collection, deposited at the Muséum Geológico of the Instituto Geológico e Mineiro (IGM, Lisbon-Alfragide), was studied, because several of the localities sampled by Paul Choffat no longer exist. Moreover, several Middle and Late Jurassic *Arcomytilus* and *Isognomon* from the Muséum National d'Histoire Naturelle at Paris were included in part of the analyses, especially for shape comparison.

With regard to lithostratigraphy, the Late Jurassic fossils from Portugal can be assigned to the Cabo Mondego [2],

Cabaços [1], Alcobaça [3], and Farta Pao formations; the latter is divided into four members (Sobral [4], Arranhó I [5], and Arranhó II [6] members), which are treated as separate units herein (Fig. 2). The terminology of the units follows Schneider et al. (2009). They have been consecutively numbered in squared brackets throughout the text and figures, corresponding more or less to their stratigraphic succession. Individual samples are denoted by the number of the stratigraphic unit and capital letters in squared brackets, according to the “code” given in the first column of Tables 1 and 2. The Oxfordian–Kimmeridgian stage boundary is interpreted *sensu gallico* herein (see Melendez and Atrops 1999 for details). The subdivision of the Kimmeridgian follows Enay (1997). The strontium isotope ages of Schneider et al. (2009) are included in Table 1 as far as available for the sampled horizons.

Table 1. Information on samples collected by the authors. From left to right: Sample abbreviations; localities and locality numbers referring to Fig. 1; GPS coordinates; inferred salinity regimes; lithostratigraphy; sampled target taxa; numerical age of horizon according to Schneider et al. (2009); assemblages or associations.

Code	Locality (numbers refer to Fig. 1)	GPS coordinates	Salinity regimes	Formation/member	Taxa	Numerical age	Assemblage/association
[1A]	Cesareda (13)	N 39°15.553 W 09°15.185	euhaline	Cabaços	<i>Isognomon</i>	155.3 ± 10	autochthonous <i>Regulifer beirensis</i> assemblage
[1B]	Cesareda (13)	N 39°15.553 W 09°15.185	euhaline	Cabaços	<i>Isognomon</i> , <i>Arcomytilus</i>	/	parautochthonous chaetetid-terebratulid- <i>Arcomytilus</i> assemblage
[1C]	Cesareda (13)	N 39°15.553 W 09°15.185	euhaline	Cabaços	<i>Isognomon</i>	/	<i>Isognomon rugosus</i> / <i>Actinostreon solitaria</i> subset
[2A]	Cabo Mondego (1)	N 40°10.690 W 08°54.300	euhaline	Cabo Mondego	<i>Isognomon</i> , <i>Arcomytilus</i>	/	<i>Isognomon rugosus</i> / <i>Actinostreon solitaria</i> subset
[2B]	Cabo Mondego (1)	N 40°10.690 W 08°54.300	euhaline	Cabo Mondego (?U)	<i>Eomiodon</i> , <i>Isognomon</i>	153.8 ± 7	<i>Isognomon rugosus</i> / <i>Eomiodon securiformis</i> subset
[2C]	Cabo Mondego (1)	N 40°10.690 W 08°54.300	euhaline	Cabo Mondego (?M)	<i>Eomiodon</i> , <i>Isognomon</i>	/	<i>Isognomon rugosus</i> / <i>Eomiodon securiformis</i> subset
[2D]	Cabo Mondego (1)	N 40°10.690 W 08°54.300	euhaline	Cabo Mondego (L)	<i>Eomiodon</i> , <i>Isognomon</i>	/	<i>Isognomon rugosus</i> / <i>Eomiodon securiformis</i> subset
[2E]	Cabo Mondego (1)	N 40°10.690 W 08°54.300	euhaline	Cabo Mondego	<i>Eomiodon</i>	/	<i>Isognomon rugosus</i> / <i>Eomiodon securiformis</i> subset
[2F]	Anção (2)	N 39°54.015 W 08°35.269	/	Cabo Mondego	<i>Isognomon</i> , <i>Arcomytilus</i>	/	isolated specimens
[3A]	Salir do Porto (3)	N 39°30.328 W 09°09.000	euhaline	Alcobaça (?L)	<i>Isognomon</i> , <i>Arcomytilus</i>	154.2 ± 4 153.6 ± 4	cf. <i>Isognomon rugosus</i> / <i>Actinostreon solitaria</i> subset
[3B]	Salir do Porto (3)	N 39°30.328 W 09°09.000	euhaline	Alcobaça (?L)	<i>Isognomon</i>	154.3 ± 4 153.4 ± 3	<i>Isognomon rugosus</i> / <i>Actinostreon solitaria</i> subset
[3C]	Salir do Porto (3)	N 39°30.328 W 09°09.000	euhaline	Alcobaça (?L)	<i>Isognomon</i>	/	<i>Isognomon rugosus</i> / <i>Eomiodon securiformis</i> subset
[3D]	São Martinho do Porto (4)	N 39°30.727 W 09°08.514	euhaline	Alcobaça (?L)	<i>Isognomon</i>	153.5 ± 3 152.0 ± 2	<i>Isognomon rugosus</i> / <i>Actinostreon solitaria</i> subset
[3E]	Barrio (6)	/	/	Alcobaça (M)	<i>Isognomon</i>	/	isolated specimens
[3F]	Consolação (12)	N 39°19.185 W 09°21.393	euhaline-brachyhaline	Alcobaça (M)	<i>Isognomon</i> , <i>Arcomytilus</i>	151.8 ± 4	Bakevellid sp. A association
[3G]	Consolação (12)	N 39°19.476 W 09°21.695	euhaline	Alcobaça	<i>Isognomon</i>	151.8 ± 4	isolated specimens
[3H]	Consolação (12)	/	/	Alcobaça	<i>Isognomon</i>	/	isolated specimens
[3I]	Consolação (12)	/	/	Alcobaça	<i>Isognomon</i>	/	isolated specimens
[3J]	Sobral da Lagoa (11)	N 39°21.382 W 09°11.036	brachyhaline-mesohaline	Alcobaça (U)	<i>Eomiodon</i> , <i>Isognomon</i>	151.8 ± 4	<i>Eomiodon securiformis</i> / nerineid sp. B association
[3K]	Vestiaría (7)	N 39°33.526 W 09°00.259	/	Alcobaça (U)	<i>Eomiodon</i> , <i>Isognomon</i>	/	isolated specimens
[3L]	Fonte Santa (8)	N 39°31.792 W 08°57.641	brachyhaline-mesohaline	Alcobaça (?U)	<i>Isognomon</i>	153.9 ± 4	cf. <i>Isognomon rugosus</i> / <i>Praexogyra pustulosa</i> subset
[3M]	Salgados (5)	N 39°32.221 W 09°07.177	/	Alcobaça (?U)	<i>Eomiodon</i> , <i>Isognomon</i>	/	isolated specimens
[3N]	Chiqueda (9)	N 39°32.567 W 08°56.745	euhaline	Alcobaça	<i>Isognomon</i> , <i>Arcomytilus</i>	154.8 ± 5 153.2 ± 3	cf. <i>Elasmotoma/Comophyllia corrugata</i> association
[3O]	S Carrascal (10)	N 39°31.976 W 09°57.575	euhaline	Alcobaça	<i>Arcomytilus</i>	153.0 ± 5	fully marine endo-/epibenthic assemblage
[4A]	A dos Arcos (19)	N 38°58.114 W 09°08.245	euhaline-brachyhaline	Sobral	<i>Isognomon</i>	150.7 ± 3	<i>Isognomon lusitanicus</i> / <i>Cylindrobullina</i> sp. subset
[4B]	Chão da Cruz (20)	N 38°58.048' W 09°06.525'	brachyhaline-mesohaline	Sobral	<i>Eomiodon</i> , <i>Isognomon</i>	149.2 ± 4	<i>Eomiodon securiformis</i> / nerineid sp. B association
[4C]	Chão da Cruz (20)	N 38°58.048' W 09°06.525'	euhaline-brachyhaline	Sobral	<i>Isognomon</i>	150.9 ± 3	<i>Isognomon lusitanicus</i> / <i>Cylindrobullina</i> sp. subset
[4D]	Chão da Cruz (20)	N 38°58.048' W 09°06.525'	brachyhaline-mesohaline	Sobral	<i>Arcomytilus</i>	/	<i>Eomiodon securiformis</i> / nerineid sp. B association
[4E]	E Arranhó (21)	N 38°57.570 W 09°07.780	brachyhaline-mesohaline	Sobral	<i>Eomiodon</i>	/	<i>Eomiodon securiformis</i> / nerineid sp. B association
[4F]	E Arranhó (21)	N 38°57.570 W 09°07.780	brachyhaline-mesohaline	Sobral	<i>Eomiodon</i> , <i>Arcomytilus</i>	150.4 ± 4	cf. <i>Eomiodon securiformis</i> / nerineid sp. B association

Code	Locality (numbers refer to Fig. 1)	GPS coordinates	Salinity regimes	Formation/member	Taxa	Numerical age	Assemblage/association
[4G]	N Nossa Senhora do Ajuda (22)	N 38°57.388 W 09°07.585	brachyhaline-mesohaline	Sobral	<i>Eomiodon</i> , <i>Isognomon</i> , <i>Arcomytilus</i>	/	cf. <i>Eomiodon securiformis</i> / nerineid sp. B association
[4H]	Santa Cruz (17)	/	brachyhaline-mesohaline	Sobral	<i>Eomiodon</i> , <i>Isognomon</i>	154.3 ± 5	<i>Isognomon rugosus</i> / <i>Eomiodon securiformis</i> subset
[4I]	Porto Dinheiro (16)	/	brachyhaline-mesohaline	Sobral	<i>Eomiodon</i>	/	cf. <i>Eomiodon securiformis</i> association
[4J]	Porto das Barcas (15)	N 39°13.754 W 09°20.362	brachyhaline-mesohaline	Sobral	<i>Eomiodon</i>	/	cf. <i>Eomiodon securiformis</i> association
[4K]	Praia de Areia Branca (14)	/	brachyhaline-mesohaline	Sobral	<i>Eomiodon</i>	/	cf. <i>Eomiodon securiformis</i> association
[5A]	Santa Cruz (17)	N 39°07.161 W 09°23.531	brachyhaline-mesohaline	Arranhó I	<i>Eomiodon</i> , <i>Isognomon</i>	150.9 ± 2	cf. <i>Arcomytilus morrisii</i> / <i>Protocardia</i> sp. nov. association
[5B]	Chão da Cruz (20)	N 38°58.048' W 09°06.525'	brachyhaline-mesohaline	Arranhó I	<i>Arcomytilus</i>	/	<i>Arcomytilus morrisii</i> / <i>Protocardia</i> sp. nov. association
[5C]	Boiero (23)	N 38°57.284 W 09°05.916	brachyhaline-mesohaline	Arranhó I	<i>Arcomytilus</i>	150.8 ± 4	<i>Arcomytilus morrisii</i> / <i>Protocardia</i> sp. nov. association
[5D]	E Arranhó (21)	N 38°57.570 W 09°07.780	brachyhaline-mesohaline	Arranhó I	<i>Arcomytilus</i>	/	<i>Arcomytilus morrisii</i> / <i>Protocardia</i> sp. nov. association
[5E]	E Mata (24)	N 38°57.935' W 09°05.848	brachyhaline-mesohaline	Arranhó I	<i>Arcomytilus</i>	/	<i>Arcomytilus morrisii</i> / <i>Protocardia</i> sp. nov. association
[6A]	Santa Cruz (17)	N 39°07.161 W 09°23.531	euhaline-brachyhaline	Arranhó II	<i>Isognomon</i>	148.5 ± 3 150.4 ± 3	parautochthonous <i>Isognomon rugosus</i> assemblage
[6B]	Santa Cruz (17)	N 39°07.161 W 09°23.531	euhaline-brachyhaline	Arranhó II	<i>Isognomon</i>	149.9 ± 3	parautochthonous <i>Isognomon rugosus</i> assemblage
[6C]	Bemposta/Serra de Alrota (25)	N 38°54.687 W 09°07.086	euhaline-(brachyhaline)	Arranhó II	<i>Isognomon</i>	/	parautochthonous <i>Isognomon rugosus</i> assemblage
[6D]	Bemposta/Serra de Alrota (25)	N 38°54.727 W 09°07.296	euhaline-(brachyhaline)	Arranhó II	<i>Isognomon</i>	147.6 ± 5	parautochthonous <i>Isognomon rugosus</i> assemblage
[6E]	Bemposta/Serra de Alrota (25)	N 38°54.700 W 09°06.906	brachyhaline-mesohaline	Arranhó II	<i>Eomiodon</i> , <i>Isognomon</i>	/	<i>Isognomon rugosus</i> / <i>Eomiodon securiformis</i> subset
[6F]	Bemposta/Serra de Alrota (25)	N 38°54.692 W 09°07.317	brachyhaline-mesohaline	Arranhó II	<i>Eomiodon</i>	/	cf. <i>Eomiodon securiformis</i> association
[6G]	Quintá (25)	N 38°58.329 W 09°14.329	euhaline-(brachyhaline)	Arranhó II	<i>Isognomon</i>	151.4 ± 4	parautochthonous <i>Isognomon rugosus</i> assemblage
[6H]	Rio Sizandro (18)	N 39°05.012 W 09°24.974	euhaline-(brachyhaline)	Arranhó II	<i>Isognomon</i>	150.1 ± 4	cf. <i>Mesosaccella dammariensis</i> / <i>Corbulomima suprajurensis</i> association
[6I]	Rio Sizandro (18)	N 39°05.012 W 09°24.974	euhaline-(brachyhaline)	Arranhó II	<i>Isognomon</i>	149.5 ± 4	cf. <i>Isognomon rugosus</i> / <i>Praeexogyra pustulosa</i> subset
[6J]	Rio Sizandro (18)	N 39°05.904 W 09°24.273	euhaline-brachyhaline	Arranhó II	<i>Isognomon</i>	149.9 ± 7	<i>Isognomon rugosus</i> / <i>Amphistrea piriformis</i> subset
[6K]	Serra de Alrota (26)	N 38°56.378 W 09°08.012	euhaline-(brachyhaline)	Arranhó II	<i>Arcomytilus</i>	150.5 ± 4	cf. <i>Mesosaccella dammariensis</i> / <i>Corbulomima suprajurensis</i> association
[6L]	Serra de Alrota (26)	N 38°56.292 W 09°07.962	/	Arranhó II	<i>Arcomytilus</i>	/	isolated specimens
[6M]	Lameiro das Antas (27)	N 38°57.389' W 09°06.906	euhaline-(brachyhaline)	Arranhó II	<i>Arcomytilus</i>	/	autochthonous <i>Arcomytilus morrisii</i> / <i>Corbulomima suprajurensis</i> assemblage
[6N]	Vila Nova (28)	/	/	?Arranhó II	<i>Arcomytilus</i>	/	isolated specimens
[6O]	SE Batalha (29)	/	/	?Arranhó II	<i>Eomiodon</i>	/	isolated specimens

From Portugal, 331 specimens of *Arcomytilus* from 36 distinct horizons (authors' collection, housed at BSPG [AC]: 19; IGM: 17) at 26 localities (AC: 16; IGM: 12), 675 specimens of *Isognomon* from 47 horizons (AC: 37; IGM: 10) at 27 localities (AC: 19; IGM: 8), and 386 specimens of *Eomiodon* from 33 horizons (AC: 19; IGM: 14) at 26 localities (AC: 13; IGM: 13) have been analysed.

The figured specimens from Portugal are deposited in the

Muséu Geológico of the Instituto Geológico e Mineiro (IGM, Lisbon) under collection numbers GML 25900-25929. Additional material is deposited in the Bayerische Staatssammlung für Paläontologie und Geologie (BSPG, Munich) under accession number 2005 V. The specimens of *Arcomytilus* and *Isognomon* from France belong to the collections of the Muséum National d'Histoire Naturelle (MNHN, Paris) and are registered under various numbers.

Table 2. Sample abbreviations, localities, inferred lithostratigraphy, and target taxa of samples from the Choffat collection at IGM (Lisbon).

Code	Locality	Formation/member	Taxa
[2G]	Cabo Mondego	Cabo Mondego	<i>Isognomon</i> , <i>Arcomytilus</i>
[2H]	Volta do Cal	Cabo Mondego	<i>Isognomon</i>
[2I]	Outeiro Pragão	Cabo Mondego	<i>Eomiodon</i> , <i>Isognomon</i>
[2J]	Valverde	Cabo Mondego	<i>Arcomytilus</i>
[2K]	Pombal	Cabo Mondego	<i>Arcomytilus</i>
[2L]	Pyramide dos Netos	?Cabo Mondego	<i>Eomiodon</i>
[2M]	São Jorge	?Cabo Mondego	<i>Arcomytilus</i>
[3P]	Fervença	Alcobaça	<i>Eomiodon</i>
[3Q]	Moinho do Barrio	Alcobaça	<i>Eomiodon</i>
[3R]	Gaieiras	Alcobaça	<i>Eomiodon</i>
[3S]	Sobral da Lagoa	Alcobaça	<i>Eomiodon</i>
[3T]	Consolação	Alcobaça	<i>Arcomytilus</i>
[4M]	Mato da Cruz	Sobral	<i>Isognomon</i>
[4N]	Mafra ao Sobral	Sobral	<i>Eomiodon</i> , <i>Arcomytilus</i>
[4O]	Fouradouro	Sobral	<i>Eomiodon</i>
[4P]	Arredores de Sirol	Sobral	<i>Arcomytilus</i>
[4Q]	Boco	Sobral	<i>Arcomytilus</i>
[4R]	Bullegueira	Sobral	<i>Arcomytilus</i>
[4S]	Forte do Sobral	Sobral	<i>Arcomytilus</i>
[4T]	São Tiago dos Velhos	Sobral	<i>Arcomytilus</i>
[4U]	Ribaldeira	Sobral	<i>Eomiodon</i> , <i>Isognomon</i>
[4V]	Silveira/Sapataria	Sobral	<i>Eomiodon</i>
[4W]	Sapataria	Sobral	<i>Arcomytilus</i>
[4X]	Silveira	Sobral	<i>Eomiodon</i>
[5F]	Mourao Senhora Ajuda	Arranhó I	<i>Arcomytilus</i>
[5G]	Mafra para Torres Vedras	Arranhó I	<i>Eomiodon</i>
[6P]	Cambelas	Arranhó II	<i>Isognomon</i> , <i>Arcomytilus</i>
[6Q]	Fortes de Alhandra	Arranhó II	<i>Arcomytilus</i>
[6R]	Santa Cruz	Arranhó II	<i>Isognomon</i> , <i>Arcomytilus</i>
[4/6A]	Cabo Espichel	?Sobral/Arranhó	<i>Eomiodon</i> , <i>Arcomytilus</i>
[4/6E]	Palheiros	?Sobral/Arranhó	<i>Isognomon</i>
[4/6F]	Ribeira	?Sobral/Arranhó	<i>Isognomon</i>
[7A]	Freixial	?Freixial	<i>Eomiodon</i>
[X1]	Cabanas de Torres	?	<i>Isognomon</i>
[X2]	Sabugueiro de Encamação	?	<i>Eomiodon</i>

Methods

Palaeoecological analysis

It is essential for the interpretation of morphological variability in fossil bivalve shells to know as much as possible about their habitat. This includes data on co-occurring organisms, community structure, and trophic webs. The macrofossil collections from the sampled horizons are qualitative in nature and do not depict relative abundance of the taxa. Nevertheless, wherever possible, the fossils from each particular horizon have been assigned to a community or association each of which is characterised by specific ecological requirements (Table 1). Most of the fossil assemblages could be assigned to distinct faunal associations as defined by Fürsich (1981a) and Fürsich and Werner (1984, 1986, 1991). For a few samples new associations had to be defined. Additionally, the microfauna and/or -facies of most of the sampled horizons were investigated briefly. From argillaceous and muddy layers sediment samples were processed by immersion in diluted hydrogen peroxide, wet-sieved down to a mesh size of 0.01 mm, dried, and picked for microfossils. From well-cemented rocks thin-sections were prepared and analysed using a binocular microscope.

Stable oxygen isotopes

Since the relationship between stable oxygen isotopes of carbonate skeletons and ambient seawater was discovered (Epstein et al. 1951), $\delta^{18}\text{O}$ analyses on carbonates have become a standard tool for reconstruction of (palaeo-) temperatures (e.g., Sharp 2007). In the present study, oxygen isotope analyses were carried out to gain additional information on the Late Jurassic palaeoclimate in Portugal; these analyses help to identify the factors that possibly influenced bivalve shell-shape. Analysis of $\delta^{18}\text{O}$ was performed on the primarily calcitic shells of the oysters *Praeexogyra*, *Actinostreon*, and *Nanogyra* from different strata across the Lusitanian Basin, and on three belemnite rostra (*Hibolites* sp.) from the Abadia Formation. All shells were previously screened for diagenesis, applying cathodoluminescence analysis and atomic absorption spectrometry. Only non-luminescent portions of clean, shiny, and translucent calcite containing < 250 ppm Mn and < 700 ppm Fe were chosen for analysis. For details on sample localities, preparation technique, and control for diagenesis see Schneider et al. (2009). Samples for stable isotope analysis were milled using an agate mortar and pestle, weighed, and measured at the laboratory of the GeoBioCenter at the Palaeontology Section of the Ludwig-Maximilians-University Munich, using a Delta plus Thermo/Finnigan MAT mass spectrometer coupled with a GasBench II preparation device. Measured values are adjusted to solid reference standards NBS-18, NBS-19, and “Pfeil” internal lab standard. Accuracy generally ranges between 0.1‰ and 0.2‰. Palaeotemperatures were reconstructed using the equation of Anderson and Arthur (1983): $T [^{\circ}\text{C}] = 16.0 - 4.14(\delta^{18}\text{O}_{\text{carbonate}} - \delta^{18}\text{O}_{\text{water}}) + 0.13$

$(\delta^{18}\text{O}_{\text{carbon}} - \delta^{18}\text{O}_{\text{water}})^2$ assuming ice free poles ($\delta^{18}\text{O}_{\text{water}} = -1.2\text{‰ PDB}$) and normal marine salinity (36 psu). The latter was evaluated by the presence or absence of stenohaline organisms (e.g., brachiopods, corals, echinoderms).

Sample preparation and measurements

After chemical and/or mechanical preparation, the length and height of all individuals of the three target taxa were measured using a calliper (measuring accuracy: 0.5 mm; Fig. 6). For *Isognomon*, the length of the ligament area and number of resilifers were recorded. Most of the specimens are incomplete and large portions of the ventral part of the shell are missing. Length, height, and thickness were recorded at the latest entirely traceable growth line. As the completeness of the valves usually varies within a single double-valved specimen, the more complete valve of each specimen was chosen for analysis. Because the umbo is commonly broken in *Arcomytilus* and *Isognomon*, measurements for length and ligament length were reconstructed for missing parts of up to 10 mm in length. Altogether, 364 valves of *Arcomytilus*, 638 valves of *Isognomon*, and 385 valves of *Eomiodon* were measured. Supplementary to the measurements, the number of ribs of *Arcomytilus* was counted in 289 valves. Counting was done along a clearly traceable growth line at about the stage of maximum shell growth (?maturity; arrow in Fig. 6A). Although several phases of slightly reduced shell growth may occur during the life of a mussel, the turning point, when growth starts to decrease substantially, can be determined quite accurately in a well-preserved, adult individual, and may represent the best point to compare rib numbers in specimens of a similar ontogenetic stage.

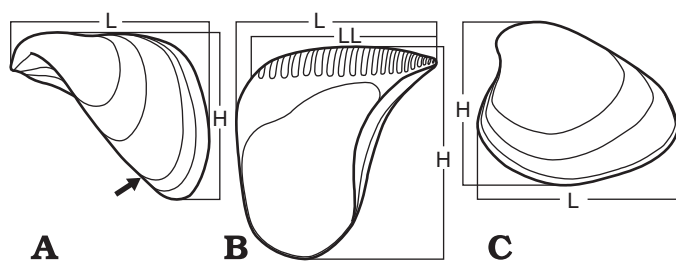


Fig. 6. Measured distances in the three target taxa. **A.** *Arcomytilus*. **B.** *Isognomon*. **C.** *Eomiodon*. Abbreviations: H, height; L, length; LL, ligament length. Arrow indicates turning point of growth.

Outline analysis

For outline analysis, specimens were oriented in such a way that the plane of the latest complete growth stage was horizontal and then photographed. Digital images were reduced to this growth stage using the rubber tool in Adobe® Photoshop CS. Subsequently, the contrast of the images was increased to obtain black and white images. The contours of the shell outlines were saved as x/y-coordinates using TpsDig 2.12 software (Rohlf 2008). In *Arcomytilus* and *Isognomon*, the tracing of x/y-coordinates was started at the umbo. In *Eomiodon*, the

centre of the lunule, which is usually more sharply defined as the umbo, was chosen as the starting point. As normalisation for size (executed by the Hangle software; see below) is included in the procedure of FFT (Fast Fourier Transformation; see details below), all coordinates registered by the software were kept for outline analysis. In total, data sets of 364 *Arcomytilus*, 561 *Isognomon*, and 321 *Eomiodon* specimens were produced.

Fourier shape analysis is a well-established method for analysing outline shape based on a combination of sine and cosine waves (Kuhl and Giardina 1982; Crampton and Haines 1996) that has been successfully tested on various biologic objects (e.g., Renaud and Michaux 2004; Bond and Beamer 2006; Liow 2006; Ponton 2006; Schulz-Mirbach and Reichenbacher 2008) including several Cretaceous and Cainozoic bivalve groups, some of which display shell shapes similar to the target taxa (Crampton and Maxwell 2000; Haines and Crampton 2000; Palmer et al. 2004; Scholz 2003; Crampton and Gale 2005, 2009; Scholz and Hartman 2007a, b). Different methods for this procedure have been developed, from which FFT was chosen because of certain advantages discussed at length by Haines and Crampton (2000). The data sets were processed using the programs Hangle, Hmatch, and Hcurve designed by Crampton and Haines (1996). The outlines were automatically smoothed (12 times) in order to eliminate pixel “noise” and insignificant outline details resulting from minor shell breakage. The numbers of harmonics that sufficiently describe the outlines were evaluated from amplitude vs. harmonic number plots according to Lestrel (1989). These plots indicated that at least seven Fourier harmonics were necessary for the analysis of *Arcomytilus*, eight for *Isognomon*, and nine for *Eomiodon*. Subsequently, the data sets were normalised for starting positions using the program Hmatch, because the outlines of all three taxa lack sharply defined homologous points. By inversion of the Fourier transformation, idealised synthetic shell outlines were generated for the first two principal components using the program Hcurve and following the approach outlined by Haines and Crampton (2000).

Statistical analyses

Height/length ratios, number of ribs, and size distribution patterns were analysed using SPSS 16.0 (SPSS Inc. 2007). All taxa were tested for correlation between the measured size parameters. In a first step, scatter plots of log transformed values of height vs. length were produced. Additionally, size was displayed in box plot diagrams where each box corresponds to one lithostratigraphic unit. The measurements are generally based on adult specimens, which can be identified by the crowding of growth lines in mature individuals (see Figs. 3–5 for examples), but also include a minor portion of juvenile or sub-adult individuals, which account for negative outliers and may enlarge the extension of the lower ranges of the boxes.

The Fourier coefficients were analysed with regard to stratigraphic, palaeoecologic, and/or taxonomic aspects applying Principal Component Analysis (PCA) based on the variance-covariance (VCV) matrix using SPSS 16.0 and PAST 1.82b software packages (Hammer et al. 2001). In order to avoid confusion caused by too many symbols, convex hulls were plotted for all samples with $N \geq 3$. Smaller samples were only included in the plots in case they enlarge the total morphospace, and thus play a role for the interpretation of the diagrams. The number of relevant principal components, i.e., those accounting for more variance than expected to be explained by random, was evaluated applying the broken stick model sensu Jackson (1993). Generally, variability was found to be best displayed in all cases by plots of PC2 vs. PC1. In neither of the analyses, PC3 helped to obtain a better decomposition of groups when plotted vs. PC1 or PC2, nor to better explain morphologic differences; thus we refrain from discussing and/or figuring these plots.

Potential evolutionary changes may be best inferred by grouping the data according to lithostratigraphy. For this purpose, plots of PC1 vs. PC2 have been constructed and groups displayed as convex hulls. Additionally, a series of artificial shell outlines was plotted on these diagrams to illustrate the morphospace of the taxa. Moreover, the confidence ellipses of group means and corresponding mean shell outlines have been produced and figured separately. In all three taxa, the lithostratigraphic groups are by far best separated by plotting the first two principal components.

In addition to lithostratigraphic grouping, Fourier coefficients were displayed in separate population plots, each representing a single time-slice or lithostratigraphic unit, in order to detect ecophenotypic adaptations and evaluate their potential relationship to biogenic and non-biogenic factors (see Supplementary Online Material [see http://app.pan.pl/SOM/app55-Schneider_etal_SOM.pdf for SOM: figs. S1–S10]). The term “population” is used herein for all specimens of a taxon derived from a single horizon. Most of these samples may not represent populations in a biological sense, but were subject to more or less distinct time-averaging (Walker and Bambach 1971; Fürsich and Aberhan 1990; Kidwell and Bosence 1991; see Fürsich et al. 2009 for details). The abbreviations used for the populations are listed in Tables 1 and 2 (column 1).

Results

In the Upper Jurassic of the Lusitanian Basin *Arcomytilus*, *Isognomon*, and *Eomiodon* range from the Middle/Late Oxfordian to the late Early Tithonian. This corresponds to approximately 10 Ma. The temporal and spatial resolution obtained by the samples used for this study and the numerical size of the individual samples enable a detailed analysis of the morphological development in these three bivalve genera with regard to evolution and/or palaeoecology. Of the six lithostratigraphic units that can be distinguished,

the Cabaços [1] (Late Oxfordian–earliest Kimmeridgian), Cabo Mondego [2] (Middle Oxfordian–Early Kimmeridgian), and Alcobaça [3] formations (Late Oxfordian–Late Kimmeridgian) do not overlap in time with the three members of the Farta Pao formation (latest Late Kimmeridgian–Early Tithonian) (Schneider et al. 2009) with regard to the sampled horizons.

Assemblages and associations

Analysis of the samples reveals a number of macrobenthic assemblages falling fully within or deviating slightly from the associations already recognised by Fürsich (1981a) and Fürsich and Werner (1984, 1986, 1991) (Table 1). The term *Isognomon rugosus* association is used also for associations containing *Isognomon lusitanicus* herein (see Systematic palaeontology section below) in order to provide palaeoecological comparability. This association is represented by several samples, attributable to at least five subsets, one of which, termed *Isognomon lusitanicus/Cylindrobullina* sp. subset, is newly described herein. This subset, recorded from the Sobral member at A dos Arcos [4A] and Chão da Cruz [4C], is composed almost exclusively of *I. lusitanicus* attaining a large size; the specimens are sparsely encrusted with *Praeexogyra pustulosa*; solitary corals (cf. *Axosmilia* sp.) may occur accessorially. The subset occurs in marly, fine-grained bioclastic sediment that contains sparse microfauna of small planispiral lituolid foraminifera, few miliolid foraminifera and several ostracod species (e.g., *Cytherelloidea* sp., *Paracypris* sp.). This assemblage together with the occurrence of two taxa of small gastropods, i.e., cf. *Cylindrobullina* sp. and a neritimorph, indicates euhaline or slightly brachyhaline salinities. In addition, *Isognomon rugosus* and *I. lusitanicus* were sampled from several horizons containing parautochthonous accumulations of disarticulated shells (termed “parautochthonous *I. rugosus* assemblage” herein).

The *Eomiodon securiformis/nerineid* sp. B association, found at Chão da Cruz [4B, D], Arranhó [4E, F], Nossa Senhora do Ajuda [4G] (all from the Sobral member [4], Farta Pao formation, Arruda Subbasin), and at Sobral da Lagoa [3J] (Alcobaça formation [3], Bombarral Subbasin), is newly defined herein. Typically, this association is dominated by *E. securiformis* and a relatively small, moderately high-coiled nerineid gastropod (nerineid sp. B of Fürsich and Werner 1986). These are frequently accompanied by large *Amauropsis* sp., *Fuersichella bicornis*, and *Anisocardia (Antiquicyprina)* sp. B (sensu Fürsich and Werner 1986). Additionally, a variety of different bivalve taxa and several corals may occur.

Several new assemblages are recorded only from single outcrops and therefore cannot be classified as associations sensu Fürsich (1981a). The autochthonous *Arcomytilus morrisii/Corbulomima suprajurensis* assemblage occurs in dark, marly clay at Lameiro das Antas [6M] (Arranhó II member [6] of the Farta Pao formation, Arruda Subbasin). It is characterised by abundant *A. morrisii* occurring in

dense clusters, by the presence of a few specimens of the large isognomonoid *Rostroperna thurmanni*, a relatively low-diversity fauna of small endobenthic bivalves dominated by *Corbulomima suprajurensis*, and a remarkably diverse echinoderm fauna (isolated skeletal elements) including common ophiuroideans.

The limestones at the Cesareda Plateau (Cabaços formation [1], Bombarral Subbasin) yielded two distinctive faunal assemblages that previously had not been encountered. The autochthonous *Regulifer beirensis* assemblage [1A] is dominated by crowded specimens of the large, thick-shelled mytilid *Regulifer beirensis*, associated in a few cases with *Isognomon rugosus* and the epibyssate pectinid *Camptonectes auritus*. Further up-section, greyish wackestones contain a parautochthonous chaetetid-terebratulid-*Arcomytilus* assemblage [1B]. Small (< 5 cm) irregularly globular chaetetid colonies, terebratulid brachiopods, and disarticulated *Arcomytilus* shells dominate the likely parautochthonous assemblage.

A few *Arcomytilus* specimens occur in a fully marine endo-/epibenthic assemblage of rather exceptional composition for the Lusitanian Basin, which is found south of Carrascal [30] (Alcobaça formation [3], Bombarral Subbasin). The fauna is predominantly composed of large burrowing anomalodesmatan (*Pholadomya*, *Ceratomya*) and heterodont bivalves, accompanied by the epibenthic reclining astarid *Coelastarte discus* (see Schneider and Werner 2007).

Several samples (termed “isolated specimens” in Table 1) consist of single or just a few specimens found isolated or within assemblages that could not be sensibly addressed. These samples often stem from less well-documented regions or time slices, and are included in the analyses to fill these gaps. Similarly, the samples from the IGM cannot be assigned to distinct faunal assemblages/associations with confidence because details on sampling procedure and species composition are lacking.

Stable oxygen isotopes

The measured $\delta^{18}\text{O}$ values range from -2.84 to 1.18 VPDB. The palaeotemperatures reconstructed from these values range from 7 to 23°C. However, in several samples that derive from brackish water environments, freshwater mixing may have significantly influenced the $\delta^{18}\text{O}$ values resulting in a deviation of several degrees from original temperature (Sharp 2007). Additionally, several samples that produced significant results for Sr-isotope stratigraphy (Schneider et al. 2009) did not yield equally significant oxygen values, as revealed by comparison of two or more samples from the same horizon. Consequently, only those values are considered for temperature reconstruction that (i) were obtained from faunal assemblages indicating fully marine conditions and (ii) are confirmed by two or more samples from the same horizon yielding similar isotope values. The palaeotemperatures reconstructed from the oyster samples suggest 16–22.5°C for the Late Oxfordian–Early Kimmeridgian (14 samples) and 15.5–19°C for the Late Kimmeridgian (5 samples). Three belemnite

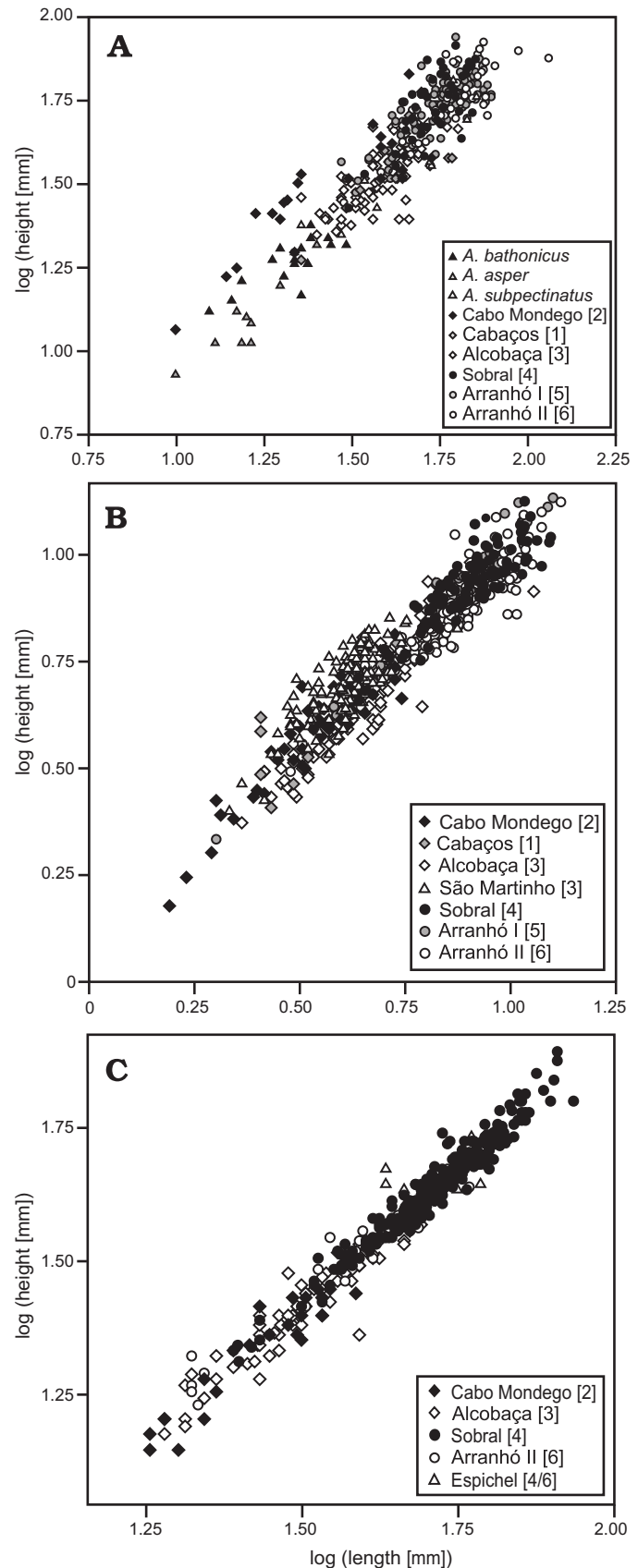


Fig. 7. Scatter plots of log transformed values of height over length for the three target taxa. A. *Arcomytilus*. B. *Isognomon*. C. *Eomiodon*. Numbers in squared brackets refer to Fig. 2.

samples from the Lower Kimmeridgian Abadia Formation yield isotope values indicating 12–14°C.

Morphometry

Size and size increase.—The height/length plots of all taxa show a distinct linear correlation (Fig. 7), which, however, is far more constant in *Eomiodon* than in *Arcomytilus* and *Isognomon*. The most obvious evolutionary process that occurs in all three genera studied is a sudden size increase (Fürsich and Werner 1986) that took place shortly after the Early/Late Kimmeridgian boundary, relatively precisely timed at ~152 Ma based on Sr isotope ages (Schneider et al. 2009). However, a distinct separation of any group is impossible based on the height/length diagrams, although the *Isognomon* specimens that are preserved as moulds (Cabo Mondego formation [2], Cabaços Formation [1], “São Martinho” [3A–D]) exhibit a slight shift to higher y-values compared to specimens of similar size that are preserved with shell (Fig. 7B). Therefore, size increase is illustrated by box plot diagrams for all genera (Fig. 8). One-way ANOVA reveals significance for *Arcomytilus* ($F_{[8; 353]} = 69.2$; $p < 0.001$), *Isognomon* ($F_{[4; 295]} = 162.8$; $p < 0.001$), and *Eomiodon* ($F_{[4; 380]} = 90.1$; $p < 0.001$) at the 0.05 level.

For specific reasons, the box-plots are based on different size parameters. All species of *Arcomytilus* in general and *Arcomytilus morrisii* in particular vary considerably in shape; often, long specimens are characterised by a relatively small height and vice versa. In order to obtain a best estimate for size, the box-plot for *Arcomytilus* is based on the log transformed geometric mean of length and height. Three boxes that display additional data sets of closely related species of *Arcomytilus* from the Jurassic of France are included in this plot. Based on a Bonferroni post hoc test, the French Bathonian species *Arcomytilus bathonicus* and *Arcomytilus asper* are distinctly smaller than *A. morrisii* from Portugal (Figs. 3, 8A). The data set of *A. pectinatus* contains scattered data and is included only to illustrate potential ancestry to *A. morrisii*, as discussed by Fürsich and Werner (1988). Within the Upper Jurassic data sets of *A. morrisii*, the samples corresponding to the Cabo Mondego [2], Cabaços [1], and Alcoaça formations [3] and the Sobral [4], Arranhó I [5], and Arranhó II [6] members are clearly separated based on the Bonferroni test ($p < 0.001$), although their whiskers show a considerable overlap of absolute sizes due to the inclusion of sub-adult specimens.

The box-plot of *Isognomon* is based on log transformed ligament length, because the thin ventral part of the shell is commonly broken off in specimens from Portugal, and corresponding measurements of shell length and height are therefore often taken from sub-adult growth stages. With exception of a few gerontic specimens that usually exhibit strongly allometric growth favouring height, ligament length is directly correlated with shell length. The plot shows a distinct gap between the boxes of the Cabo Mondego [2] and Alcoaça formations [3] (no specimens with shell preservation

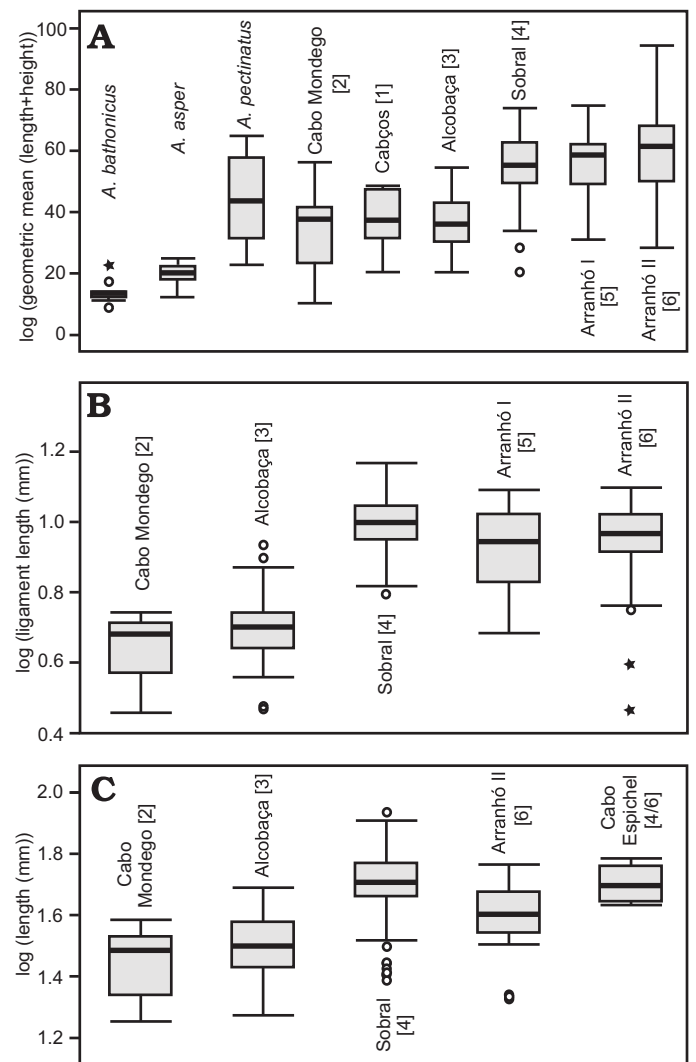


Fig. 8. Box plots of size for the three target taxa. **A.** Size of *Arcomytilus* based on log transformed geometric means of length and height. **B.** Size of *Isognomon* based on log transformed ligament length. **C.** Size of *Eomiodon* based on log transformed shell length. Arrangement of boxes corresponding more or less to their stratigraphic succession, from left to right. Numbers in squared brackets refer to Fig. 2.

could be obtained from the Cabaços Formation [1]) and those of the different members of the Farta Pao formation [4, 5, 6] (Fig. 8B), which is confirmed to be significant by a Bonferroni post hoc test ($p < 0.001$). Again, the whiskers indicate a considerable overlap of absolute sizes, which may, however, in this particular case be due largely to juvenile specimens (especially for the Arranhó I [5] and Arranhó II [6] members). The few positive outliers from the Alcoaça formation [3] that prevent the total separation of the two groups based on size of adult specimens were collected from a single horizon at Consolação [3F]. With regard to lithostratigraphy, this horizon is attributed to the Upper Oxfordian–Upper Kimmeridgian Alcoaça formation. However, sample [3F] is positioned near the top of this formation and Sr-isotope data indicate a Late Kimmeridgian age, which appears to post-

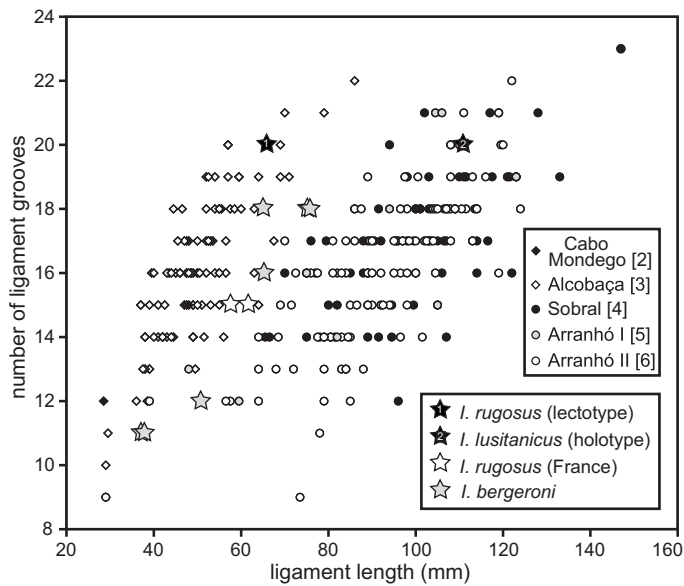


Fig. 9. Scatter plot of resiliifer number over ligament length in *Isognomon*. The two groups that correspond to lithostratigraphy are clearly visible. Numbers in squared brackets refer to Fig. 2.

date the onset of size increase. Based on these considerations, *Isognomon* from the Upper Jurassic strata of the Lusitanian Basin may be separated into two chronostratigraphically distinct size groups, Oxfordian–Lower Kimmeridgian and Upper Kimmeridgian–Tithonian, based on ligament length. Remarkably, the same horizon [3F] yielded a considerable number of *Arcomytilus* shells that clearly belong to the group of minor size. Certainly, size increase occurred within a distinct time span but not absolutely simultaneous in different bivalve taxa.

In *Eomiodon*, size increase is also evident, but occurs less abruptly than in *Arcomytilus* and *Isognomon*. The samples stem from four units only (Cabo Mondego [2] and Alcobaça [3] formations and Sobral [4] and Arranhó II [6] members). The exclusively carbonate rocks of the Cabaços Formation [1] and the Arranhó I member [5] formed under conditions most likely unsuitable for *Eomiodon*. A sample of the Choffat collection at the IGM from Cabo Espichel is treated separately in this analysis, as it cannot be assigned to one of the Farta Pao members with confidence. Although *Eomiodon* may casually be subject to moderately allometric changes during ontogeny, these modifications are not clearly displayed in the height/length ratio; consequently, size is relatively accurately displayed by length, and the plot is based on log transformed values of this parameter (Fig. 8C). The Bonferroni post hoc test confirms a significant separation of the Cabo Mondego [2] and Alcobaça [3] samples from those of the Farta Pao formation ($p \leq 0.002$). Apart from the taxa studied herein, a more or less contemporary intraspecific or intrageneric size increase can be observed in several other bivalve taxa from the Lusitanian Basin (e.g., *Jurassicorbula* spp., *Coelastarte discus*, *Myophorella* spp.; FTF, SS, WW

personal observations), indicating that this process is fairly widespread.

Resiliifer density in *Isognomon*.—In *Isognomon*, the step in size increase co-occurs with a substantial change in resiliifer density that is displayed in an additional scatter plot of the number of resiliifers against ligament length (Fig. 9). Naturally, this plot is only based on specimens with shell-preservation. Although a few outliers exist, two groups that correspond to the Late Oxfordian–Early Kimmeridgian (Cabo Mondego [2] and Alcobaça [3] formations; Group I) and the Late Kimmeridgian–Early Tithonian (Farta Pao formation [4, 5, 6]; Group II) can be relatively clearly separated based on the plot. Sample [3F] is represented by a single specimen in this plot, as all other specimens from this sample are articulated, and the number of resiliifers cannot be counted; this single specimen, however, plots within Group I (as do four other specimens from the Farta Pao formation). The change in resiliifer density occurs as follows: While total size and respective ligament length rise, the number of resiliifers stays constant, and thus the number of resiliifers per cm decreases. Based on these observations, a separation of *Isognomon* from the Late Jurassic of Portugal into two chronologically different species seems evident. Including data from the figured type specimens of *Isognomon rugosus* (Münster, 1835) and *Isognomon lusitanicus* (Sharpe, 1850) these specimens clearly resemble the two groups of resiliifer density. Consequently, Group I may be correctly identified as *I. rugosus* (Münster, 1835), while for Group II the original identification as *I. lusitanicus* (Sharpe, 1850), considered by Fürsich and Werner (1989a) as a synonym of *I. rugosus*, is re-established (for details on the taxonomy, see Systematic palaeontology section below). Several specimens from the Upper Jurassic of France, deposited at the MNHN and labelled *Isognomon rugosus* and *Isognomon bergeroni*, respectively, are positioned next to the right margin of the *rugosus*-group, but still are included therein.

Rib numbers in *Arcomytilus*.—In *Arcomytilus*, the total number of radial ribs represents an additional parameter that

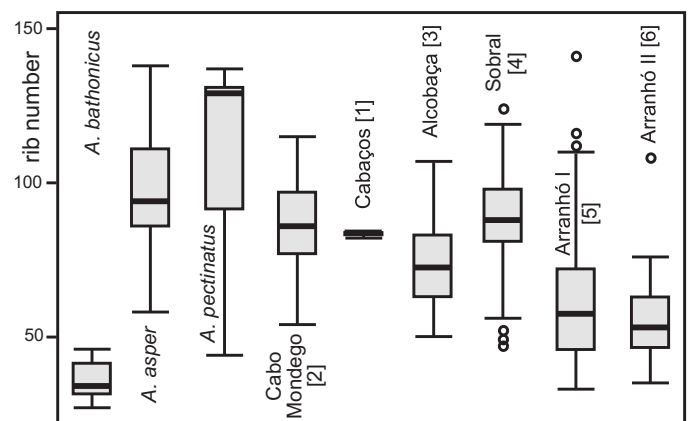


Fig. 10. Box plot of rib numbers in *Arcomytilus*. Numbers in squared brackets refer to Fig. 2.

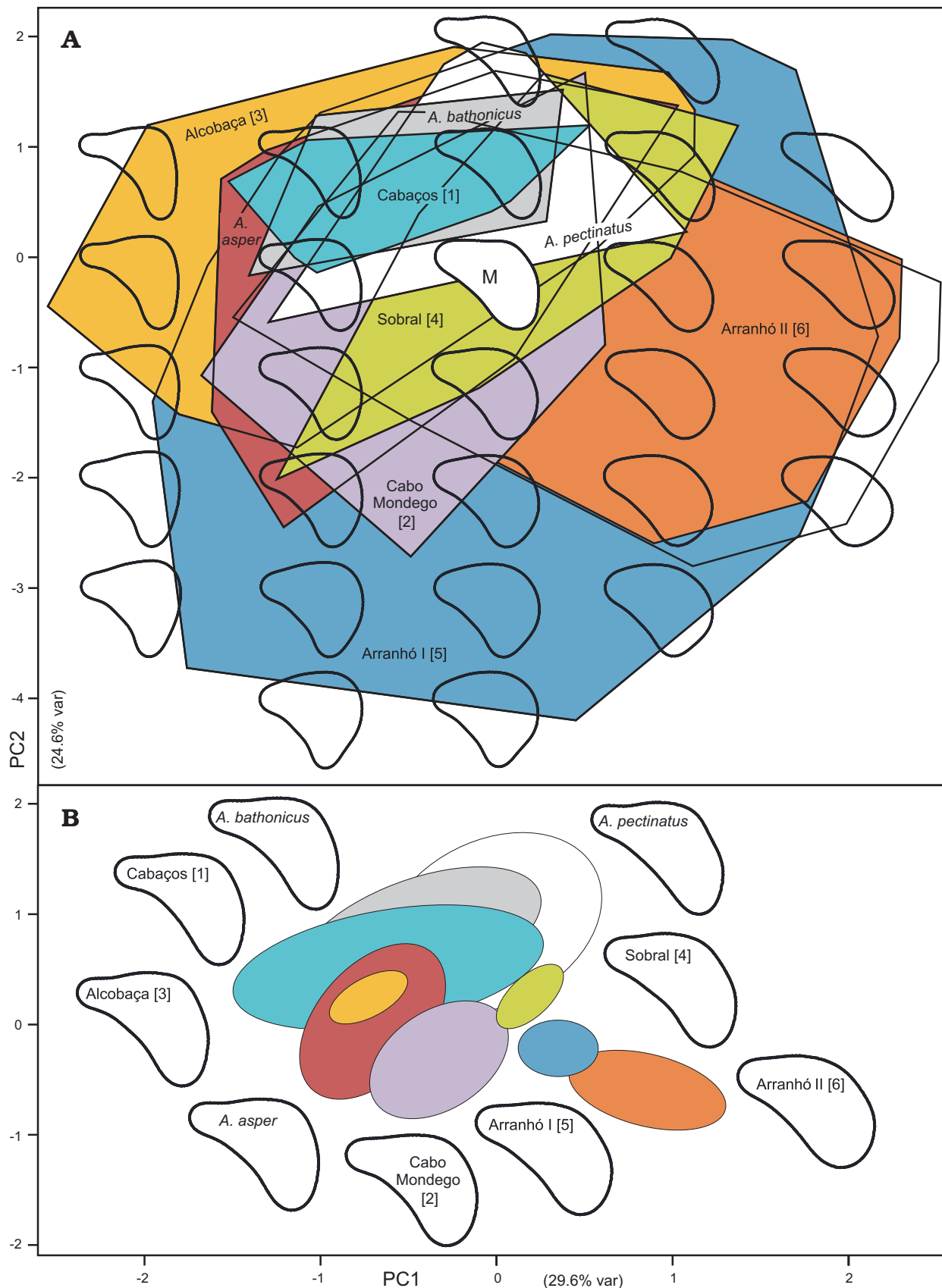


Fig. 11. Lithostratigraphy plot of *Arcomytilus*. **A.** Different species and lithostratigraphically grouped *Arcomytilus morrisii* are displayed as convex hulls. Calculated artificial shell outlines for full number coordinate pairs are plotted to illustrate the morphospace. M; mean artificial shell outline. **B.** 95% confidence ellipses of group means and corresponding calculated shell outlines for group means are plotted. Numbers in squared brackets refer to Fig. 2.

Table 3. Number of shell outlines and percentage of explained variance of principal components 1–3 for PCA plots in Figs. 9–11 and S1–S10.

Genus	Category	N	% var PC1	% var PC2	% var PC3	% cum var
<i>Arcomytilus</i>	lithostratigraphy	476	29.6	24.3	12.6	66.5
	Cabo Mondego, Cabaços, Alcobaça	100	33.0	16.2	14.4	63.6
	Sobral	43	38.8	14.8	12.5	66.1
	Arranhó I, Arranhó II	158	31.5	23.1	12.5	67.1
<i>Isognomon</i>	lithostratigraphy	722	35.4	15.5	11.5	62.4
	Alcobaça	111	33.3	16.0	13.4	62.7
	moulds: Cabo Mondego, Cabaços, Alcobaça	170	30.7	18.1	11.9	60.7
	Sobral	99	28.9	17.0	15.4	61.3
	Arranhó I, Arranhó II	174	29.5	20.0	9.5	59.0
<i>Eomiodon</i>	lithostratigraphy	480	36.4	18.4	10.3	65.1
	Cabo Mondego, Alcobaça	71	44.8	16.9	8.1	69.8
	Sobral	221	39.8	15.4	10.0	64.2
	Arranhó II	26	29.9	19.1	13.0	62.0

may be utilised to infer evolutionary changes. Whereas *Arcomytilus bathonicus* and *Arcomytilus asper*, co-occurring in Upper Bathonian sediments at Luc-sur-Mer (Calvados, France), can be separated clearly based on rib numbers (Fig. 10), *Arcomytilus asper*, *Arcomytilus pectinatus*, and *Arcomytilus morrisii* from Portugal cannot be distinguished from each other by this method. Interestingly, the specimens from the Cabo Mondego formation [2] are significantly different from those from the Arranhó I [5] and Arranhó II [6] members based on one-way ANOVA ($F_{[8; 286]} = 23.1$; $p < 0.001$)

and a Bonferroni post hoc test ($p < 0.001$), while they show similar rib numbers ($p = 1.0$) to those from the Sobral member [4] (Fig. 10). All in all, a largely continuous, gradual decrease of rib numbers from the Upper Bathonian *A. asper* to the Oxfordian to Kimmeridgian *A. pectinatus* and across the whole range of *A. morrisii* is inferred and a clear separation of two or more groups of *Arcomytilus* from the Upper Jurassic of Portugal based on rib numbers is impossible. Moreover, an increase in rib number in specimens from the Upper Kimmeridgian Sobral member [4] is against the trend.

Shell outline shape.—Height/length plots for the three bivalve genera clearly show that apparent morphological variability of the shells cannot be sufficiently displayed by such a simple method (Fig. 7). The same holds true for any other combination of linear measurements tested, including inflation, ligament length or height, or absolute shell thickness. In contrast, the PCA plots of Fourier coefficients display the major part of information on shell outline shape retained in the analyses. In all analyses, not more than the first three principal components are relevant based on broken stick analysis (Jackson 1993), and the first one (PC1) accounts for $\geq 29\%$ of total variance. Cumulative variance of PC1–3 generally ranges between 59 and 70%. The percentages of explained total variance for PC1, PC2, and PC3 in all PCAs are listed in Table 3.

In *Arcomytilus*, the total range of shape variability of *A. morrisii* expands notably with time and size. Slender, sub-elliptical or tapering forms that dominate the stocks of the older strata and also the three species from the Middle and Upper Jurassic of France are joined by broadened or high sub-triangular

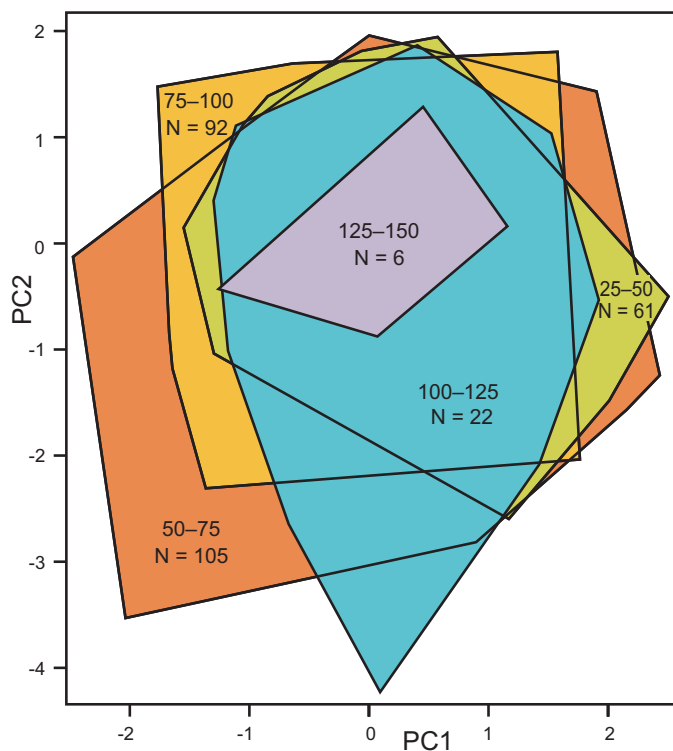
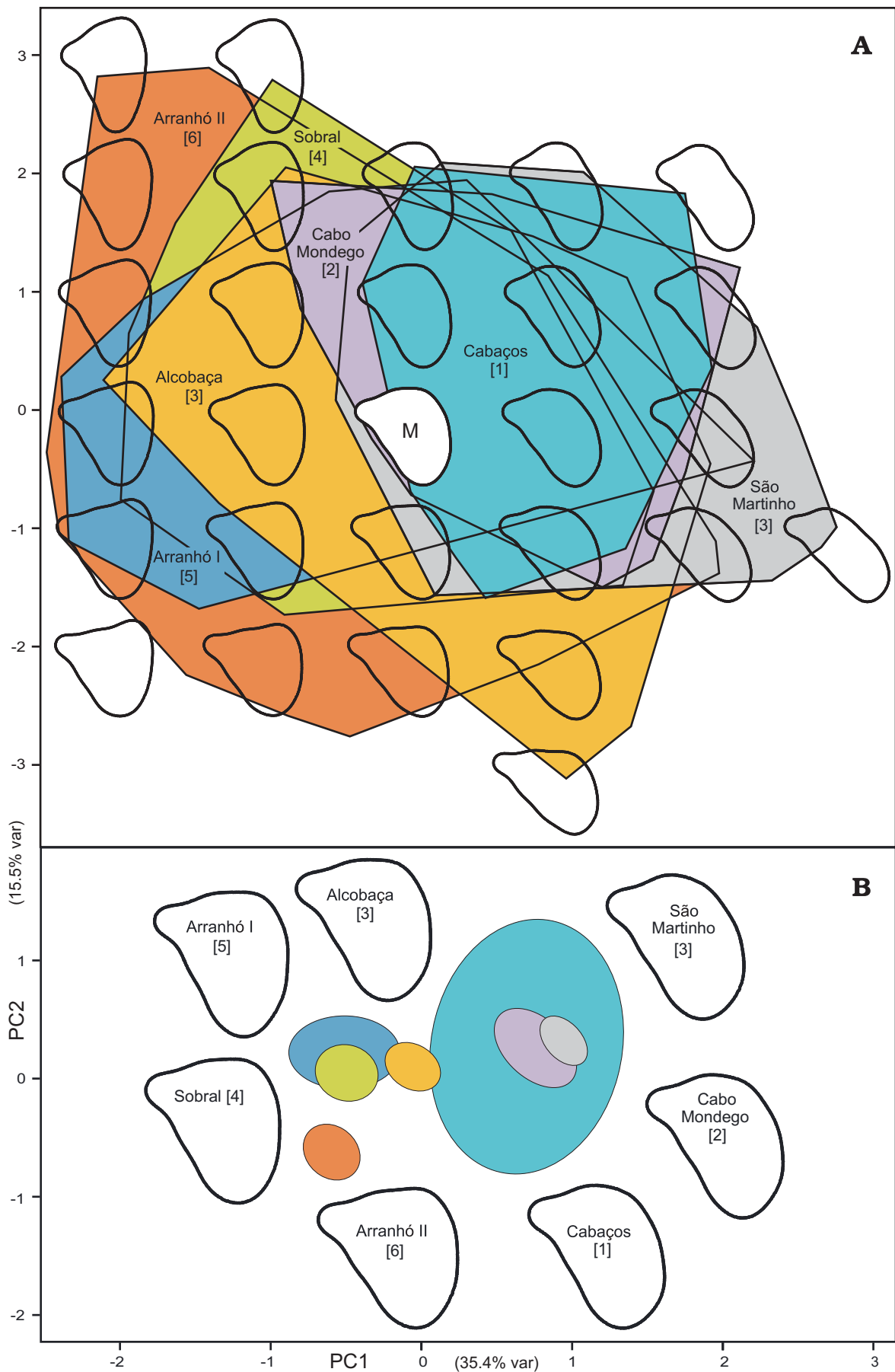


Fig. 12. PCA plot of shell shape in *Arcomytilus*, grouped according to rib number in steps of 25 ribs and displayed as convex hulls.

Fig. 13. Lithostratigraphy plot of *Isognomon*. **A.** Lithostratigraphically arranged groups are displayed as convex hulls. Calculated artificial shell outlines for full number coordinate pairs are plotted to illustrate the morphospace. **M.** mean artificial shell outline. **B.** 95% confidence ellipses of group means and corresponding calculated shell outlines for group means are plotted. Numbers in squared brackets refer to Fig. 2.



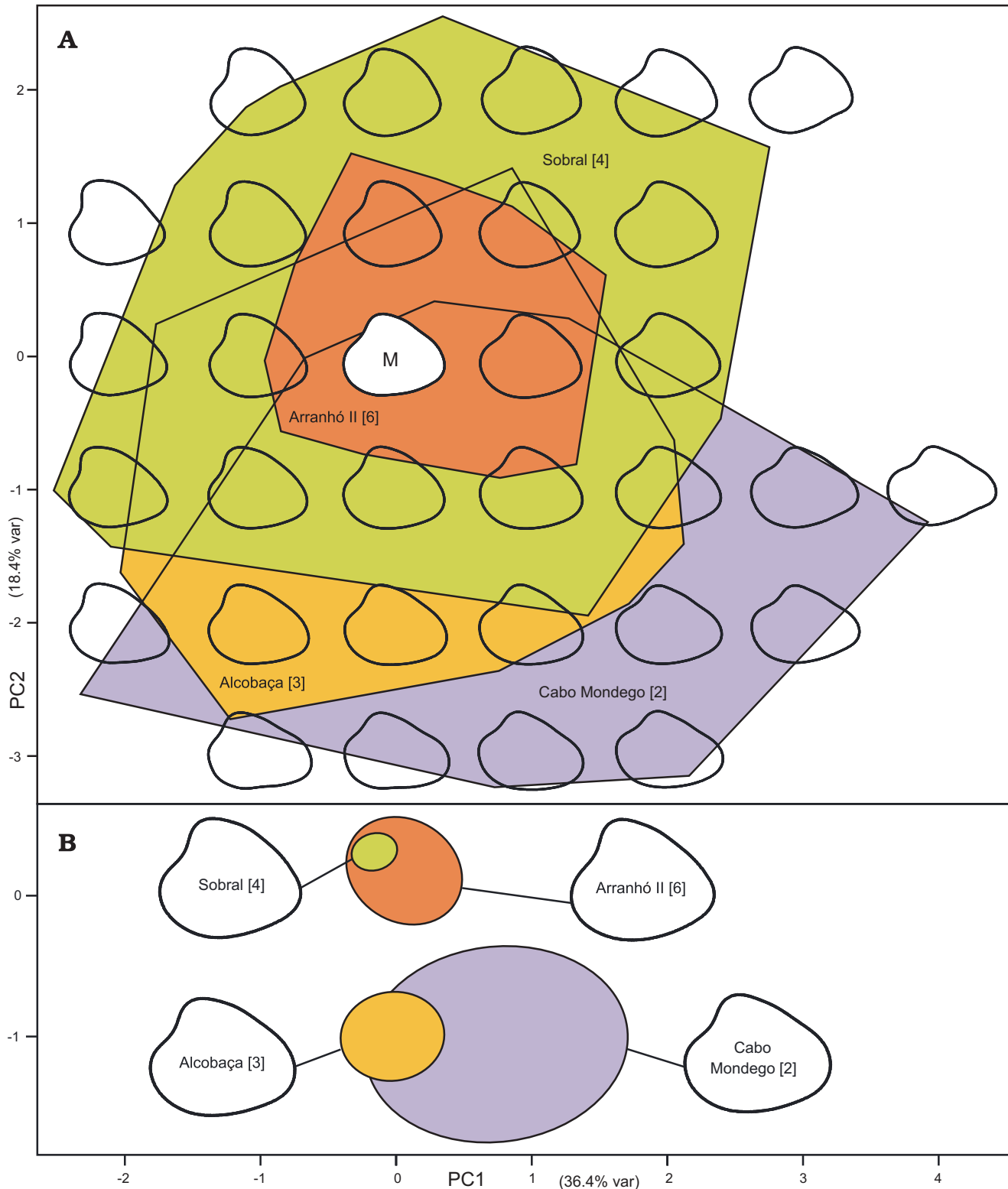


Fig. 14. Lithostratigraphy plot of *Eomiodon securiformis*. **A.** Lithostratigraphically arranged groups are displayed as convex hulls. Calculated artificial shell outlines for full number coordinate pairs are plotted to illustrate the morphospace. M, mean artificial shell outline. **B.** 95% confidence ellipses of group means and corresponding calculated shell outlines for group means are plotted. Numbers in squared brackets refer to Fig. 2.

shells in the Arranhó I [5] and Arranhó II [6] members (Fig. 11A). All convex hulls overlap considerably, rendering a sensible separation of any group impossible. As can clearly be in-

ferred from the plot, shape and size are not correlated, since the morphospace occupied by the large specimens from the Sobral member [4] is largely included in those spanned by the

small Cabo Mondego [2] and Alcobaça [3] specimens. Almost the entire morphospace of *Arcomytilus morrisii* is covered by the specimens from the Arranhó I member [5]. The ellipse plot of group means shows variability at a fairly small scale (Fig. 11B). A truly consecutive tendency of shape change is interrupted by the specimens from the Alcobaça formation [3], which plot between the group means of the stratigraphically older Cabaços [1] and Cabo Mondego [2] formations. It should be noted that the low number of seven harmonics readily describes the general differences in shell shape, but does not capture shape details of the umbo, which are quite different among species and lithostratigraphic groups. Generally, *Arcomytilus morrisii* is characterised by tapering, pointed, slender umbones, while these are much blunter in *Arcomytilus bathonicus*, *Arcomytilus asper*, and *Arcomytilus pectinatus* (Fig. 3). Additionally, specimens of *A. morrisii* from the Cabaços [1] and Cabo Mondego [2] formations typically have slightly more blunt umbones than the individuals from younger strata.

In order to evaluate the relationship between rib number and shell shape, the Fourier coefficients are displayed in a separate plot grouped by rib number, with each group comprising a 25 ribs interval. The plot shows large to complete overlap and almost identical centres of all five convex hulls, and a separation of any group is not indicated (Fig. 12).

In *Isognomon*, a separate group of shell outlines, termed “São Martinho”, has been included in the lithostratigraphy PCA plot (Fig. 13). The data gathered in this group comprise two large samples from the coastal outcrops at São Martinho do Porto and Salir do Porto that form a single horizon exposed at either end of the cove. Based on lithology and Sr isotope data, these outcrops are assigned to the Alcobaça formation (Schneider et al. 2009). However, as nearly all specimens from the Cabo Mondego and Cabaços formations, these *Isognomon* are preserved as partial moulds. Since the aragonitic inner part is much thickened at the anterior side of an *Isognomon* shell due to shell weighting (compare Seilacher 1984) the thin outer calcitic layer has been compressed and imprinted onto the internal mould when the aragonite was dissolved during diagenesis. As a result, the shell outlines are artificially shortened (as can also be seen from the height/length plot) and cannot be directly compared to specimens in full shell preservation. However, the shell outlines of the partial moulds can still be compared among different samples with similar preservation. The convex hulls of specimens from the Cabo Mondego [2] and Cabaços [1] formations and from São Martinho [3A–D] display almost complete overlap (Fig. 13A). Despite the shortening artefact that results in a shift towards higher PC1 values, all three groups show more than 50% overlap with the convex hulls of groups with shell-preservation, suggesting that originally there was no major difference in the occupied morphospace. Additionally, the convex hulls of groups with preserved shell overlap to a large degree (Fig. 13A) while group means, except that of Arranhó II [6], are almost equal (Fig. 13B) and thus a sepa-

ration of the previously defined Groups I and II, indicated by ligament length and resiliifers per cm, cannot be deduced from shell outline shape. Moderately increased shape variability including specimens with a more triangular shell outline (indicated by declining PC1 values), more tapering beaks (decreasing PC2 values), and higher ligament area (increasing PC2 values) is displayed by the younger and larger shells from the Farta Pao formation.

Eomiodon displays somewhat less variability than the other genera, not only with regard to size but also shape (Fig. 14A). Moreover, separation of different lithostratigraphic groups based on shell outline shape is impossible. The convex hulls of specimens from the Alcobaça [3] and Sobral [4] formations overlap to a great extent. The Arranhó II [6] group occupies a relatively small area in the centre of the Sobral morphospace [4] and is nearly entirely included in the Alcobaça group [3]. In contrast to *Arcomytilus* and *Isognomon*, where shape variability increases with time, the largest variability in *Eomiodon* is observed in the stratigraphically oldest specimens from the Cabo Mondego formation [2]. The latter group includes several more elongated specimens (decreasing PC2 values) either with well-projecting, strongly prosogyrous (decreasing PC1 values) or slightly elevated, almost central beaks and a narrow, slightly tapering posterior shell (increasing PC1 values). Its convex hull overlaps only for about 50% with the others. In contrast, specimens from the Alcobaça formation [3] and Sobral [4] and Arranhó II [6] members have rather uniform, relatively high and short shell outlines with markedly prosogyrous umbones, relatively straight ventral margin, and a generally more equal-sided triangular shape. The confidence ellipses of the latter two group means are almost concentric. The ellipses of the Alcobaça and Cabo Mondego formations are centred slightly below (Fig. 14B).

Three population plots for different lithostratigraphic units or time slices have been produced from the Fourier coefficients of *Arcomytilus* (SOM: figs. S1–S3), four of *Isognomon* (SOM: figs. S4–S7), and another three of *Eomiodon* (SOM: figs. S8–S10). In all of these plots, individual populations show large areas of overlap, and the convex hulls of large samples generally span a major part of the total morphospace. In a few cases, particular samples exceed the total morphospace in a certain direction. For example, *Arcomytilus* populations [4R] and [4T] in SOM figure S2 include straight, elongated specimens that extend the morphospace towards higher PC1 and PC2 values. In SOM figure S8, the morphospace of the Salgados *Eomiodon* population [3M] enlarges towards lower PC1 and PC2 values due to a single, strongly elongated, gerontic individual. However, no population is clearly separated from all others in any of the plots.

Samples assignable to the same faunal associations may occupy a similar morphospace, e.g., *Arcomytilus* populations [4D, 4F] that belong to the *Eomiodon securiformis*/nerineid sp. B association (SOM: fig. S1), and *Eomiodon* samples [6E, 6F] from merely identical environments that are as-

signed to an almost monospecific *Eomiodon securiformis* association (SOM: fig. S10). Conversely, other populations that belong to identical associations share only part of the morphospace. Although both *Isognomon* samples are assigned to the *Isognomon lusitanicus/Cylindrobullina* sp. subset and come from similar facies in the same area of the Arruda Subbasin, population [4C] in SOM: fig. S6 includes a number of more slender, elongated shells, while the stout, sub-rectangular forms included in sample [4A] are absent and vice versa. Moreover, samples assigned to different associations may occupy congruent morphospace parts. While [4B] and [4F] in SOM: fig. S9 represent *Eomiodon* populations from the *Eomiodon securiformis/nerineid* sp. B association, and population [4H] stems from an almost monospecific *E. securiformis* association, the respective convex hulls overlap to a large degree.

Although all convex hulls show a large area of overlap, *Isognomon rugosus* samples from the Arruda Subbasin in SOM: fig. S7 are dominated by stout shells with high and rounded ligamental areas, while populations from the coastal sections also include more slender and more triangular specimens. In both regions, populations with a similar morphospace belong to different associations and subsets and come from different facies, e.g., [5A] from carbonate rocks and [6J] from sandy marl.

Discussion

Evolutionary implications

Size increase.—Several potential causes may trigger size increase in bivalves. In the authors' opinion, increasing nutrient supply and enhanced primary productivity is the most likely scenario in the case of the Upper Jurassic Lusitanian Basin, as other factors can be neglected or considered at least highly unlikely.

(1) Evolutionary size increase, commonly known as Cope's Rule, has been recorded for various groups of organisms including Jurassic bivalves (Hallam 1975, 1998; Johnson 1994) and is regarded as "a genuine evolutionary phenomenon" (Hallam 1975: 493) in those animals. Usually, increasing body size of bivalves is correlated with a decline in population size that is limited by the available food resources (Hallam 1998). However, all studied taxa from Portugal formed dense populations up to the Tithonian, as can be inferred from in situ preserved bivalve populations. Moreover, the examples discussed by Hallam (1975, 1998) and Johnson (1994) display a slow (several million years) and gradual size increase, whereas in the taxa from Portugal this process occurs relatively rapidly and in a punctuated pattern, and thus is not evolutionary in the sense of Cope's Rule, but is rather controlled by one or more environmental factors. A similar case is reported by Johnson (1999), dealing with size reduction in Bathonian bivalves. As a result, evolutionary size increase may be a common phenomenon in various organisms

but obviously has to be tested for each particular case (e.g., Gould and MacFadden 2004).

(2) The major change from a carbonate to a siliciclastic regime in the Lusitanian Basin directly followed an episode of intense rifting (Rasmussen et al. 1998; Alves et al. 2002) and occurred around the Oxfordian–Kimmeridgian transition (Leinfelder and Wilson 1998). It therefore clearly predates the size increase seen in the bivalves. Anyway, size seems to be independent of facies, as both small and large specimens of all three genera are recorded from carbonate and siliciclastic horizons.

(3) All three taxa generally flourished in brackish waters, but also occurred under more or less fully marine conditions. However, the composition of the different associations is largely driven by salinity (Fürsich and Werner 1984, 1986), and the appearance of identical associations during both time intervals in the Lusitanian Basin excludes salinity as a factor delimiting size.

(4) During the Late Jurassic, Portugal was situated close to the northern tropics (Smith et al. 1994; Blakey 2007) and generally characterised by summer-wet tropical climate and minor seasonal temperature fluctuations, as suggested by general circulation models (Sellwood and Valdes 2006). Moreover, no major climatic changes during the Late Jurassic are evident from this area and estimated mean land-surface temperature based on climate models is around 30°C (Sellwood and Valdes 2006), while sea-surface temperatures range between 20–30°C (Valdes and Sellwood 1992; Moore et al. 1992). Reconstructed palaeotemperatures based on oxygen isotope data from the Portuguese Upper Jurassic are somewhat lower than these predictions and range between 12–14°C based on belemnites and 15.5–22.5°C based on oysters, which is close to the temperatures calculated from belemnites of Kimmeridgian and Tithonian age from Mallorca (14–16°C; Price and Sellwood 1994). Generally, both belemnites (e.g., McArthur et al. 2007a, b; Wierzbowski and Joachimski 2007) and oysters (Kirby et al. 1998; Surge et al. 2001, 2003) are thought to precipitate calcite with $\delta^{18}\text{O}$ in close equilibrium with ambient sea-water. An offset of 2–5°C for belemnites and oysters from the same horizon may be explained by different life style (nektonic versus benthic) and is in good accordance with data gathered from similar taxa from various other regions and time-slices (e.g., Anderson et al. 1994; Wierzbowski 2002; Wierzbowski and Joachimski 2007). The total ranges of temperature values for the Late Oxfordian–Early Kimmeridgian and Late Kimmeridgian–Early Tithonian do not vary significantly, which argues against temperature affecting size increase.

(5) The local sources and directions of freshwater run-off may have been largely constant during the Kimmeridgian and Tithonian as major rifting had already ceased at the end of the Late Oxfordian (Leinfelder and Wilson 1998; Rasmussen et al. 1998; Alves et al. 2002). Due to fairly constant climatic conditions (see previous paragraph), no prominent changes in weathering should have occurred. Consequently, major changes in sea water chemistry resulting from fresh-

water run-off most likely can be disregarded. Possibly, freshwater discharge into the subbasins that formed during the Late Jurassic due to the diapiric rise of salt pillows (Wilson et al. 1989; Alves et al. 2002, 2003) may have originated from different sources, causing slight differences in water chemistry. However, both small and large bivalve forms occur in two or more subbasins. Thus, local and spatial variations in water chemistry as documented by a carbonate versus siliciclastic sedimentation regime obviously did not affect size in the bivalves. Extensive sea floor spreading in the Tagus Abyssal Plane during the Late Jurassic (Wilson et al. 1989; Alves et al. 2006) may have influenced sea water chemistry (inorganic carbon; e.g., Katz et al. 2005) in the region. However, the partial isolation of the Lusitanian Basin from the open sea renders this scenario unlikely.

(6) Potentially, bivalve size increase may have been triggered by an elevated and more stable food supply, which means higher phytoplankton productivity (Johnson 1994, 1999 and references therein; Perez Camacho et al. 1995). As most bivalves are filter-feeders, they profit more directly from such an increase than, for example, browsing gastropods or echinoderms, which do not show a substantial size increase in the basin during the same time interval (cf. Vermeij 1990). A global increase of phytoplankton productivity during the Late Jurassic is indicated by increasing $\delta^{13}\text{C}$ ratios (Katz et al. 2005; Martin et al. 2008). Whether the Lusitanian Basin was affected by this tendency in spite of its poor connections to the Proto-Atlantic cannot be proven. We have measured $\delta^{13}\text{C}$ ratios of the oyster shells used for palaeotemperatures reconstruction. However, these values are influenced by too many factors (e.g., vital effects, salinity) that cannot be controlled exactly and thus do not allow sound conclusions.

We suggest that progradation of basin infill and continental environments, respectively, may have resulted in an increased nutrient supply by freshwater run-off from these areas into the diminishing marginal marine environments within the Lusitanian Basin. This hypothesis is corroborated by a considerable increase in the diversity and abundance of Dasycladales, Foraminifera, and Ostracoda during the Late Kimmeridgian and Tithonian (Ramalho 1971).

Morphological changes.—Besides size, shell shape is the second important parameter that may yield even more information on the life of a bivalve. As reported above, all target taxa exhibit considerable variability in shell outline. Trying to explain these differences, the life style of the bivalves has to be considered. *Arcomytilus*, like most Mytilidae, exhibits an anteroventral gape; although this is not a true byssal gape (Mikkelsen and Bieler 2008), it may be inferred from this structure that the bivalves were fixed to the substrate by byssal threads (Cox et al. 1969). Usually, mytilids fix to hard substrates (rocks, hardgrounds, shells) or (bio-)clasts on sand or gravel bottoms (e.g., Tebble 1966; Stanley 1972; Poppe and Goto 1993). Apart from minor morphological modifications for adaptation to an irregularly shaped surface, these individuals are commonly characterised by a straight antero-ventral

shell margin (Stanley 1972), as seen in most specimens of *Arcomytilus asper*, *Arcomytilus bathonicus*, and *Arcomytilus pectinatus*, and also in many *Arcomytilus morrisii*. The latter species, however, acquired a partially semi-infaunal, endo-byssate life-style, settling on soupy sediment (Fürsich 1980), similar to Quaternary *Brachidontes* from Argentina (Aguirre et al. 2006) and many other extant and fossil mytiliform bivalves (Stanley 1972). The tapering beaks of these forms were buried within the sediment, while the antero-ventral portion of the shell formed a large flat surface resting on the sea bottom. Both adaptations helped to stabilise the bivalve in growth position.

A triangular shape, relatively thin shell (the latter cannot be proven for specimens from the Jurassic of Portugal, because of limited preservation quality), and possibly also a larger size may be advantageous in quiet lagoonal settings, as observed for extant *Mytilus* (Akester and Martel 2000). Moreover, an individual may have a better access to the water column if it develops a more triangular shell, and thus may have an advantage when competing for food. In favourable environments, *Arcomytilus morrisii* formed dense populations, usually in the form of large clusters composed of numerous individuals, similar to modern *Mytilus edulis* (which is, of course, notably smaller and strictly epibyssate) on tidal flats of the modern North Sea (SS personal observation).

An additional cause for shape variability in *Arcomytilus* may have been competition for space (Leinfelder 1986; Aguirre et al. 2006). Usually, the bivalve clusters are composed of individuals of the same generation and therefore of almost equal size. As all individuals grow at about the same rate, space may have become limited within the cluster, causing irregularly shaped shells that enforce growth towards non-occupied patches of the seafloor. However, mytilids generally can cast off and replace byssal threads allowing for limited mobility (Cox et al. 1969). This may explain why individuals of even extreme shapes have normal proportions. Moreover, influence of competition for space on shape variability in modern *Mytilus* is low (Akester and Martel 2000), and thus may have been also of minor importance in *Arcomytilus* shells.

The reasons for shape variability in *Isognomon* may be similar to those in *Arcomytilus*. The genus *Isognomon*, defined by an edentulous hinge in adulthood and by the presence of a multivincular ligament with slender, narrowly and equally spaced resilifers (Muster 1995; Tëmkin 2006) and most likely polyphyletic (Tëmkin 2006), displays a large variety of shell shapes and strategies of byssal attachment (Printrakoon and Tëmkin 2008). Several species of *Isognomon* acquired adaptations to life on soft substrates. Large, thin-shelled modern species, e.g., the “mudflat *Isognomon*” of Printrakoon and Tëmkin (2008), may form epibyssate clusters that are all fixed to a single, horizontally aligned individual of *Isognomon*. A similar life style may be discussed for *Isognomon rectangularis* that occurs sympatric with *Isognomon lusitanicus* at a few localities of the Arranhó II member in the central Lusitanian Basin. In contrast, *Isognomon*

rugosus and its descendant *I. lusitanicus* had an endobyssate life style, fastened to bioclasts within soft sediment (Fürsich 1980), similar to several species of *Isognomon* (*Hippochaeta*) from the Cainozoic of Europe (“orthothetic edge-wise recliners”; Seilacher 1984). However, *Isognomon* (*Hippochaeta*) *maxillatus* (Lamarck, 1801) from the Mediterranean Pliocene likely achieved stabilisation almost entirely by weighting of the hinge area and by its byssus (Savazzi 1995); it lacks the broadened anterior shell surface that is well-developed in most specimens of *Isognomon rugosus* and *Isognomon lusitanicus* and helped them to attain a stable position lying on the sediment surface. Consequently, in the latter two species only the umbonal area may have penetrated the sediment, as suggested by the strongly forward projecting umbones commonly seen in *I. rugosus* and *I. lusitanicus* and by the gradual realignment of the ligament axis for an angle of up to 30° in gerontic individuals (Fig. 4C).

Unlike *Arcomytilus morrisii* and particular modern *Isognomon* species, *Isognomon rugosus* and *Isognomon lusitanicus* did not form clusters, but rather occurred in dense banks composed of live specimens of various growth stages but also containing dead shells. These banks may have extended for hundreds of square meters, as can be observed in the Sobral member at the Atlantic coast south of Santa Cruz (Fürsich et al. 2009). Large variability in shell shape and the development of strongly triangular morphs may also have been triggered by competition for food and related upward growth as inferred for *Arcomytilus*.

The multivincular ligament of *Isognomon* is composed of fibrous sublayers that fill the resilifers and lamellar sublayers that are placed between the resilia and connect the fibrous parts (Tëmkin 2006). In some samples from Portugal, part of the fibrous material is still preserved. Measurements of several specimens show that ligamental planes of opposing valves form a maximum angle of ~50° in the central part of the ligament length, while angles are much narrower (~30°) at the anterior and posterior portions of the ligament. These values are constant throughout ontogeny, which must have been achieved by constant shell thickening in the sub-ligamental region. Evaluating the thickness of the lamellar ligament portions, the valves may have been gaping with a maximum angle of ~25° in live specimens. Whether less numerous but broader resilifers provided an adaptive advantage, e.g., with regard to strength or physiological costs, cannot be clarified based on fossil material.

The slight decrease of shell elongation that occurs in *Eomiodon* through time (Fig. 14) may be related to size increase. As can be inferred from shell characters, *Eomiodon* is a shallow-infaunal filter feeder. Consequently, increase in size and respective body mass may have caused a relative decrease in muscle strength of these bivalves (Stanley 1970, 1972). As a result, shortened shells, which would have had to burrow less deeply to attain their growth position with the posterior end just below the sediment-water interface, may represent an advantageous adaptation in large *Eomiodon*.

Ecophenotypy

It can be generally stated that ecophenotypy between associations or populations can not be proven based on the samples analysed in this study. On one hand, even among the exceptionally large dataset used for this study, many samples are too small to be statistically significant, and thus do not allow the use of more sophisticated statistical methods. On the other hand, intraspecific shape variability seen in all three taxa usually occurs within populations and thus may be driven by synecological factors. This pattern becomes obvious in most of the population plots (SOM: figs. S1–S10), as small samples are commonly included in the morphospace of the largest samples from a particular time slice or lithostratigraphic unit.

In *Arcomytilus* the sampled populations may be assigned to nine different associations or assemblages representing euhaline to mesohaline conditions. However, no distinct shape modification occurs, that could be linked to salinity or faunal composition. A single relatively small population, i.e., [6M] from the Arranhó II member [6] that is assigned to the autochthonous *Arcomytilus morrisii*/*Corbulomima suprajurensis* assemblage, stands out, due to its extremely small shape variability (SOM: fig. S3). Unfortunately, no other samples from this widespread assemblage are available, as well-preserved specimens from the more or less unconsolidated mud-facies are extremely hard to obtain. Two additional samples that occupy a similar, small morphospace [5F, 6Q] come from the Choffat collection and cannot be assigned to a particular ecological group. The same is true for samples [4R] and [4T] that include somewhat aberrant, more straight and slender specimens than the other populations from the Sobral member [4] (SOM: fig. S2).

To a certain extent, the high variability seen in *Arcomytilus* from the Arranhó I [5] and Arranhó II [6] members may reflect ecophenotypy. In the aforementioned strata, the preferred habitat of *Arcomytilus morrisii* were soft or even soupy sediments in shallow lagoonal settings, either siliciclastic or calcareous in nature. All populations from these soft bottom settings include a major portion of moderately to strongly curved and/or broadened, triangular shells, while the contemporaneous more sandy, less soupy facies of the Sobral member [4] were inhabited by less variable populations of common shape. As already outlined, broad, triangular shells may be advantageous in calm water habitats (Akester and Martel 2000). Moreover, the increase of shell surface in these broadened specimens may have rendered a purely epibyssate mode of life rather inconvenient. As a result, a semi-infaunal life style has been adapted in the respective settings, as indicated by specimens with tapering, curved beaks.

Results from rib density analysis show clearly that an adequate temporal and spatial sample density is indispensable for disentangling true evolutionary trends and ecophenotypic plasticity. An evolutionary trend towards fewer ribs is suggested by the data from all units in the Lusitanian Basin—with exception of the specimens of *Arcomytilus* from

the Sobral member [4] (Fig. 10). In the samples from this member, an increase in rib numbers argues against the general trend. Moreover, rib numbers are obviously not correlated with adult shell size, as many small adults from, e.g., the Cabo Mondego and Alcobaça formations tend to have even more ribs as numerous large shells from younger strata. Ribs may bifurcate or additional ribs may become inserted at any growth stage. Commonly, these processes occur periodically, but often also punctually even on a single shell, without any identifiable fixed pattern. This renders a substantial effect of numbers and strength of ribs on shell stability unlikely. Moreover, shell shape has no influence on rib density (Fig. 12). However, there must be an adaptive value of high, respectively low, numbers of ribs. Potentially, rib density may be linked to the substrate. Less numerous but somewhat more prominent ribs may be advantageous in soupy sediments (carbonate mud in Arranhó I [5] or silty clay in Arranhó II [6] members), possibly to stabilise the individuals in the sediment, while the specimens settling on the silty to fine-sandy sediments of the Sobral Member may have benefited from more numerous, less elevated ribs in any way. Whether less numerous ribs represent a hydrodynamic advantage in quiet settings, and vice versa, remains to be tested. This is, however, beyond the scope of this study.

Ecophenotypy in *Isognomon rugosus* can clearly be negated. All larger samples show similar, modest variability with regard to shell shape and more or less produced umbones (SOM: figs. S4, S5), although they come from two assemblages and four different associations, one of them with four distinct subsets. As a result, shell form is influenced by individual competition for space and food and likely by small-scale variations in substrate rather than by any other environmental parameter. A similar degree of variability is displayed by *Isognomon lusitanicus* that come from four associations and three subsets (Table 1). Occasionally, single populations, though showing large areas of overlap in their convex hulls, may develop slightly different gross shapes (SOM: figs. S6, S7). However, these variations cannot be correlated with ecological features with certainty and samples from different associations may well fill a similar morphospace, while samples from the same subset may occupy slightly disparate positions in the plots. For example, all populations from localities of Arranhó I [5] and Arranhó II [6] members at the Atlantic coast tend to include more triangular shells with pointed beaks, while rectangular forms with short beaks dominate in populations from the Arruda subbasin. However, all of these populations overlap for a large part of their morphospace and there is no evidence from these data that supports the existence of geographic subspecies in statu nascendi, although geographical isolation in the subbasins may have occurred. As similar geographically isolated and ecologically stressed environments are known to cause frequent rapid speciation (e.g., Müller et al. 1999; Harzhauser and Mandic 2008), at least some attention should be paid to this hypothesis.

In *Eomiodon*, a significant correlation between shell shape and environmental conditions could not be detected. More-

over, shape variability is generally low within certain time-slices and lithostratigraphic units. From Fig. 14B and SOM: fig. S8, it becomes obvious that relatively few individuals are responsible for the greater morphospace occupied by *Eomiodon* from the Cabo Mondego formation [2]. The two large populations from the Alcobaça formation [3] show almost equal variability and largely cover the shape variability of smaller samples. However, no palaeoecological data exist for the large samples. Slight differences in shape variability among populations can be inferred from the Sobral member [4] (SOM: fig. S9). However, populations from both the *Eomiodon securiformis* association and the *Eomiodon securiformis/nerineid* sp. B association include specimens of similar shape within and between populations (SOM: fig. S9) and differences between samples from similar or different associations are more or less equal. Hence, there is no indication for ecophenotypy in *Eomiodon*.

Systematic palaeontology

The systematic arrangement of higher taxa follows Mikelsen and Bieler (2008), while ranks are adopted from Amler (1999).

Class Bivalvia Linné, 1758

Infraclass Autolamellibranchiata Grobben, 1894

Subclass Pteriomorphia Beurlen, 1944

Order Mytiloidea Férussac, 1822

Superfamily Mytiloidea Rafinesque, 1815

Family Mytilidae Rafinesque, 1815

Genus *Arcomytilus* Agassiz in Sowerby, 1842

Type species: Mytilus pectinatus Sowerby, 1821. Weymouth, Dorset, S England, Kimmeridge Clay, Kimmeridgian.

Remarks.—The genus *Arcomytilus* was proposed by Agassiz in a note on *Mytilus pectinatus* Sowerby, 1821, included in the German translation of the *Mineral Conchology of Great Britain* in 1842 (p. 318). James Sowerby had already passed away by that time. Nevertheless, he has to be cited as author of this publication, and the arrangement of authorities given by Soot-Ryen (1969) is correct.

Arcomytilus morrisii (Sharpe, 1850)

Fig. 3A–F.

1850 *Mytilus morrisii*, n. s.; Sharpe 1850: 187, pl. 22: 5a, b.
 1866 *Mytilus morrisii* Sharpe; de Loriol and Pellat 1866: 89, pl. 9: 1, 2.
 1868 *Mytilus morrisii* Sharpe; de Loriol and Cotteau 1868: 187, pl. 13: 9.
 1872 *Mytilus morrisii* Sharpe; de Loriol et al. 1872: 335, pl. 19: 2.
 1988 *Arcomytilus morrisii* (Sharpe, 1850); Fürsich and Werner 1988: 123–125, text-figs. 10–12, pl. 4: 5–10.

For extensive synonymy and description see Fürsich and Werner (1988).

Type locality: Not designated; “between Sobral and Torres Vedras” (Sharpe 1850); western Arruda subbasin.

Type horizon: “limestone of the subcretaceous series”; presumably

Arranhó I member of Farta Pao formation (Upper Kimmeridgian/Lower Tithonian).

Original diagnosis.—“Shell falciform, with an elevated keel dividing the valves into two very unequal portions, the posterior gibbose and rounded, the anterior excavated, and nearly perpendicular to the plane which separates the valves; with the exception of a small smooth space near the beak on the anterior side, the valves are covered with numerous rounded bifurcating ribs, crossed by concentric lines, which latter are most strongly marked on the anterior side; the ribs on the posterior side are coarse, and radiate from the beak; those on the anterior side rise from the keel, and are much finer than the others: beaks pointed and terminal.” (Sharpe 1850).

Remarks.—The holotype of *Arcomytilus morrisii* figured by Sharpe (1850) represents a large, fully grown, typical specimen of this species. Consequently, the comprehensive original diagnosis matches the appearance of the species quite accurately. However, as discussed above, a large variability of shell shapes exists. As noted by Fürsich and Werner (1988), some specimens of *A. morrisii*, especially from Oxfordian and Lower Kimmeridgian strata in Portugal, closely resemble *Arcomytilus pectinatus* (Sowerby, 1821) (Fig. 3I). Additionally, morphometric analyses revealed affinities to *Arcomytilus bathonicus* (Fig. 3H) and *Arcomytilus asper* (Fig. 3G) (which are, however, distinctly smaller) of several specimens of *A. morrisii*. However, all of these species are quite variable in shape and several other nominal species of Jurassic *Arcomytilus* closely resemble certain specimens from Portugal. On one hand, these problems may indicate that the genus is in need of a comprehensive revision. On the other hand, morphological species concepts in extant Mytilidae have been proven to be insufficient in smooth (*Mytilus*: Gosling 1992a, b; Gardner 2004; *Bathymodiolus*: Maas et al. 1999) and ribbed (*Brachidontes*: Lee and Ó Foighil 2004, 2005; Aguirre et al. 2006) representatives, suggesting that a separation of fossil species may also be difficult in many cases. Similar results were achieved by a morphometric study using complex measurements for outline description of Devonian mytiliform bivalves (Hajkr et al. 1960). Of course, a typically-shaped individual of *Arcomytilus morrisii* can be distinguished easily from a typically-shaped *A. pectinatus* shell. Knowledge of typical shape and shape variability of a species, however, requires the possibility to study large populations, preferably from several localities. Based on the more than 300 specimens from Portugal included in this study, *A. morrisii* is regarded a valid species that can, in most cases, be clearly distinguished from *A. pectinatus* or other similar species. Typical *A. morrisii* specimens are characterised by a relatively slender elongated shape, tapering, often curved beaks, a rounded postero-ventral margin (in *A. pectinatus*, it is angularly truncated or even incurved in gerontic specimens), and a coarser and more irregular ribbing pattern than in other species.

Most likely, *A. pectinatus* invaded the Lusitanian Basin soon after the establishment of marginal marine environments in the Middle Oxfordian. Possibly due to geographical

isolation, *A. morrisii* evolved from the former species in the basin, while *A. pectinatus* persisted in other shallow areas of the Western European epicontinental seas. Presumably, *A. morrisii* spread from central Portugal into northern and central France during the Tithonian, as it has been recorded in these regions with largely typically-shaped specimens from strata of that age (de Loriol and Pellat 1866, de Loriol and Cotteau 1868; de Loriol et al. 1872).

Order Pterioida Newell, 1965

Superfamily Pterioidea Gray, (1820) 1847

Family Isognomonidae Woodring, (1828) 1925

Genus *Isognomon* Solander in Lightfoot, 1786

Subgenus *Isognomon* Solander in Lightfoot, 1786

Type species: *Ostrea perna* Linné, 1767 “in Indiis”, Indian Ocean; Recent.

Remarks.—Four species of *Isognomon* (*Isognomon*) from Upper Jurassic strata in the Lusitanian Basin can be distinguished. Two of these species, i.e., *I. (I.) promytiloides* Arkell, 1933 and *I. (I.) rectangularis* Fürsich and Werner, 1989, represent epibyssate forms with relatively flat, laterally compressed valves and only weakly prosogyrous beaks. These taxa are not further discussed herein, as they have been described adequately by Fürsich and Werner (1989a).

Two other *Isognomon* (*I.*) species from the Lusitanian Basin that were held to be synonymous by Fürsich and Werner (1989a) are adapted to an endobyssate, semi-infaunal life style. The multivincular ligament of these taxa is usually situated in 14 to 19 resilifers in adult shells. Specimens with 12 to 23 resilifers may occur. Initial rapid shell and ligament growth decreases gradually with the bivalve attaining maturity. In gerontic specimens, total shell growth had nearly ceased, while the ligament area still increased in height. Nevertheless, the angle between the ligament surfaces in left and right valves is constant during ontogeny.

Isognomon (Isognomon) rugosus (Münster, 1835)

Figs. 4A, F, H, 19A, B, E–G.

1835 *Perna rugosa* sp. nov.; Münster in Goldfuss 1835: 105, pl. 108: 2b only.

1952 *Isognomon (Isognomon) bergeroni* (Bigot Mss) sp. nov.; Chavan 1952: 23, pl. 1: 39–42.

1986 *Isognomon rugosus*; Fürsich and Werner 1986: fig. 24.

1989a *Isognomon (Isognomon) rugosus* (Münster, 1835); Fürsich and Werner 1989a: 123–125, text-fig. 12, pl. 8: 2 only.

?2002 *Isognomon (Isognomon) rugosum* (Münster in Goldfuss, 1835); Delvene and Fürsich 2002: 200, pl. 1: 3.

?2007 *Isognomon (Isognomon) rugosum* (Münster, 1835); Delvene 2007: 14, pl. 1: 7.

non 2007 *Isognomon (Isognomon) rugosus* (Münster, 1835); Schneider and Werner 2007: p. 135, fig. 8A–C.

For extensive synonymy and description see Fürsich and Werner (1989a).

Type locality: Not designated; “Weserkette”, Lower Saxony/Westphalia, NW Germany.

Type horizon: “In dark Jurassic limestone and the underlying ferruginous sandstone” (translation of Münster in Goldfuss 1835); ? Heersumer Schichten, ? Lower Oxfordian.

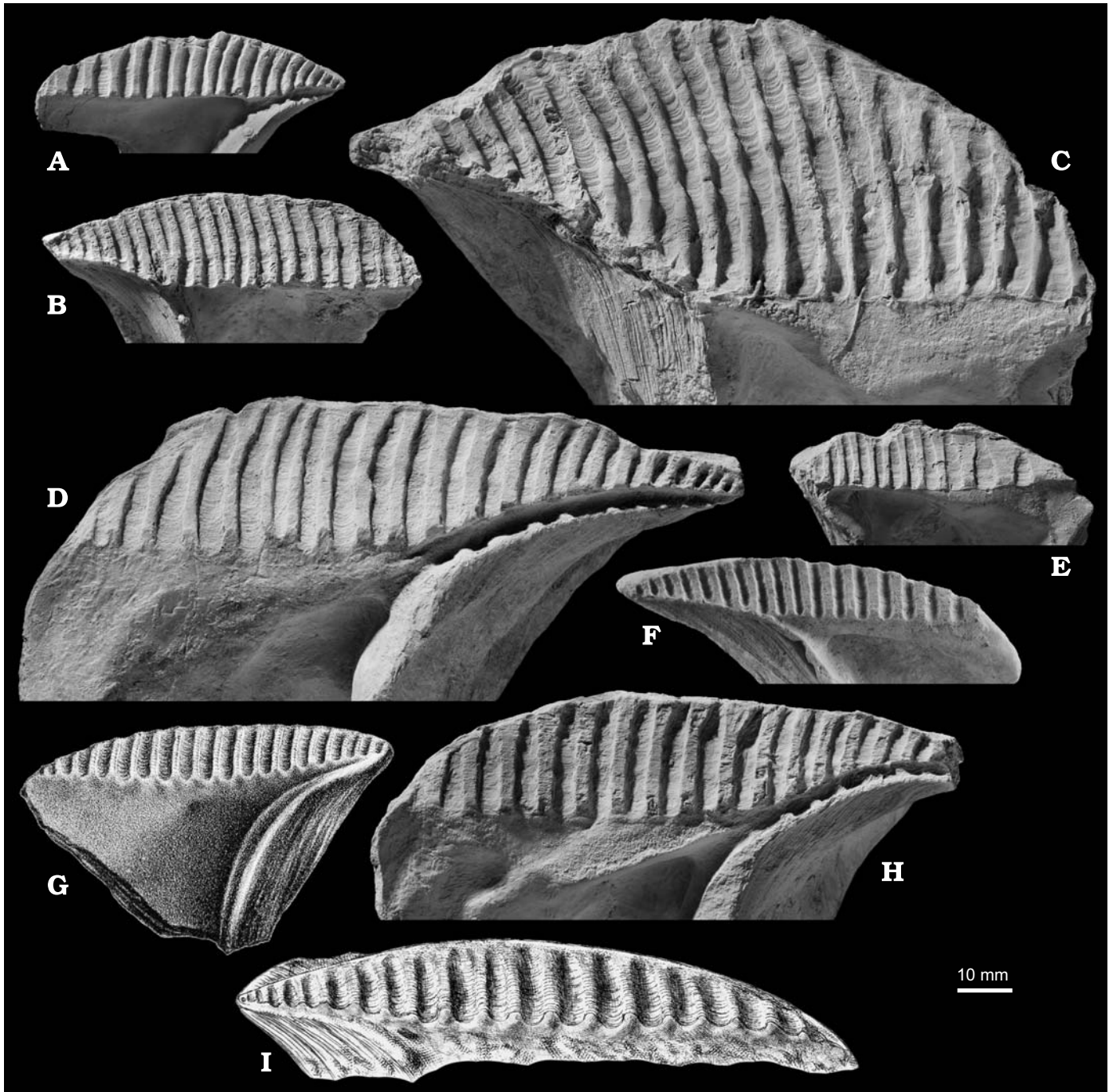


Fig. 15. Ligament arrangement in isognomonid bivalve *Isognomon* from the Upper Jurassic of Portugal, France, and Germany. **A, B, E–G.** *Isognomon rugosus* (Münster in Goldfuss, 1835). **C, D, H, I.** *Isognomon lusitanicus* (Sharpe, 1850). **A.** Left valve with typical arrangement of resilifers. Early Kimmeridgian, Alcobaca formation, Fonte Santa. GML 25923. **B.** Right valve of a gerontic individual with fusion of two resilia due to incurvature and space reduction. Early Kimmeridgian, Alcobaca formation, Fonte Santa. GML 25924. **C.** Right valve. Gerontic specimen with extremely high ligament area and markedly incurved resilifers. Late Kimmeridgian, Sobral member, Santa Cruz. GML 25925. **D.** Left valve with slightly irregular resilifers and dorsal margin. Early Tithonian, Arranhó II member, Bemposta/Serra de Alrota. GML 25926. **E.** Right valve. Irregular specimen with broadened resilifers and resilia in posterior part. Early Kimmeridgian, Alcobaca formation, Fonte Santa. GML 25927. **F.** Right valve labelled “*Isognomon bergeroni* (Bigot)”; Late Oxfordian, Astartien, Sables de Glos, Calvados, France; MNHN A33500. **G.** Left valve. Lectotype. Reproduction of drawing in Goldfuss (1826–44: pl. 108: 2b). **H.** Left valve with typical arrangement of resilifers. Early Tithonian, Arranhó II member, Bemposta/Serra de Alrota. GML 25928. **I.** Right valve. Holotype. Reproduction of drawing in Sharpe (1850: pl. 23: 8).

Original diagnosis.—“*Perna* testa subrhomboidea dorso convexa anguloso-rugosa in alam depressam producta, umbo-

nibus prominentibus, margine cardinali abliquo, canaliculis (18) subarcuatis.” (Münster in Goldfuss 1835).

Emended diagnosis.—Thick-shelled, antero-ventrally inflated, small- to medium-sized *Isognomon* (maximum ligament length ~70 mm) with subtrigonal, subrhomboidal, or subrectangular shell outline, strongly prosogyrous, tapering beaks, and an average of 3.3 resilifers per centimetre ligament length.

Remarks.—Fürsich and Werner (1989a) provided a detailed description of this species, which, besides the indication of size, accurately matches the displayed shell characters. The designated lectotype (Fürsich and Werner 1989a) figured by Münster in Goldfuss (1835: pl. 108: 2b), could not be detected either at the Goldfuss Museum, Bonn or at the BSPG, and must therefore be considered lost. The figure shows the inner side of a fragment of a left valve, including the ligamental area and a large portion of the anterior margin (Fig. 15G). Completeness of the ligamental area cannot be clearly inferred from the figure. The posterior and ventral part of the shell (more than 50% of the original size) is missing. The lectotype plots well with Group I, when included in the resilifer density plot (Fig. 9). This largely holds also true of several specimens of “*Isognomon bergeroni*” from the Sables de Glos (Fig. 15F; Late Oxfordian in age; Buffetaut et al. 1985) in western France investigated at the MNHN in Paris. However, the specimens of *Isognomon rugosus* from the Tithonian of northern and central France figured by de Loriol and Pellat (1866, 1874–75), also largely plot with *I. rugosus* from Portugal (Fig. 9), suggesting that this species may have survived in France, and *Isognomon lusitanicus* (see below) may represent a form endemic to the Lusitanian Basin. Thus, measurements based on figures from old monographs should be taken with care, as, often due to printing demands, the magnification of figured specimens may deviate distinctly from that given in the figure captions.

Isognomon (Isognomon) lusitanicus (Sharpe, 1850)

Figs. 4B–E, G, I, 19C, D, H, I.

1850 *Perna lusitanica*, n.s.; Sharpe 1850: 189–190, pl. 23: 7, 8.

1986 *Isognomon rugosus*; Fürsich and Werner 1986: fig. 24.

1989a *Isognomon (Isognomon) rugosus* (Münster, 1835); Fürsich and Werner 1989a: 123–125, text-figs. 12, 13, pl. 8: 1, 6, 7, pl. 12: 7, pl. 18: 2, pl. 20: 3.

2007 *Isognomon (Isognomon) rugosus* (Münster, 1835); Schneider and Werner 2007: 135, fig. 8A–C.

Type locality: Not designated; “between Enxarra dos Cavalheiros and San Sebastian, and between Sobral and Torres Vedras” (Sharpe 1850), western Arruda subbasin.

Type horizon: “subcretaceous limestone”; presumably Sobral member of the Farta Pao formation (Upper Kimmeridgian/Lower Tithonian).

Original diagnosis.—“Subrhomboidal, very thick and heavy, marked irregularly by the lines of growth: anterior side deeply depressed, and sloping inwards; posterior side slightly rounded away towards the palleal margin: cardinal margin arched. Hinge-areas very broad, receding one from another, and projecting anteriorly: ligamental hollows long and numerous, broader than the intervening spaces, and slightly increasing in width posteriorly, about twenty-four in number in a large specimen. Valves very thick, especially

towards the hinge; space occupied by the animal nearly rectangular and very small in proportion to the whole shell. Right valve larger and thicker, and with a deeper hinge-area than the left.” (Sharpe 1850).

Emended diagnosis.—Thick-shelled, antero-ventrally inflated, medium- to large-sized *Isognomon* (ligament length usually 80–125 mm in adults) with subtrigonal, subrhomboidal, or subrectangular shell outline, strongly prosogyrous, tapering beaks, and an average of 1.8 resilifers per centimetre ligament length.

Remarks.—The original diagnosis of Sharpe (1850) characterises the species quite well. Hence, none of the studied specimens exhibits 24 resilifers. Only 10 out of 189 valves with completely preserved ligament area yield more than 20 resilifers, with a maximum of 23 resilifers in a single specimen. Moreover, a marked asymmetry between left and right valves as proposed by Sharpe (1850) could not be detected. The type specimen of Sharpe (1850) (Fig. 15I) plots well with Group II, when included in the resilifer density plot (Fig. 9).

Except with respect to size, the description of the shell of *Isognomon rugosus* in Fürsich and Werner (1989a) matches exactly with the characters found also in *Isognomon lusitanicus*. Generally, *I. lusitanicus* can be easily distinguished from *I. rugosus* by its substantially larger size in adulthood, and, most strikingly, by the average number of resilifers per centimetre, which is by 1.5 lower than in *I. rugosus*. Consequently, *I. lusitanicus* must be considered a valid species. Additionally, the two species occur in different time intervals (*I. rugosus*: Late Oxfordian–Early Kimmeridgian; *I. lusitanicus*: Late Kimmeridgian–Early Tithonian). We infer that *I. lusitanicus* evolved in the Lusitanian Basin from *I. rugosus* during the Kimmeridgian, approximately 152 Ma ago. To date, *I. lusitanicus* has not been recorded from outside the Lusitanian Basin, and is considered as endemic.

Subclass Heteroconchia Hertwig, 1895

Superorder Heterodonta Neumayr, 1883

Order Veneroida H. Adams and A. Adams, 1856

Superfamily Arcticoidea Newton, 1891

Family Neomiodontidae Casey, 1955

Genus *Eomiodon* Cox, 1935

Type species: *Astarte libanotica* Fraas, 1878. Dakún, Lebanon, “Sandsteinformation” (Sandstone Formation), Cenomanian.

Eomiodon securiformis (Sharpe, 1850)

Fig. 5A–H.

1850 *Cyprina securiformis* n. s.; Sharpe 1850: 182–183, pl. 22: 1–3. non 1860 *Cyprina securiformis* Contej.; Contejean 1860: pl. 26: 10, 11. 1986 *Eomiodon securiformis*; Fürsich and Werner 1986: 324, fig. 24. 1994 *Eomiodon securiformis*; Fürsich 1994: 343, fig. 24A.

Type locality: Not designated; “between Sobral and Torres Vedras and also about three miles south-west of Alenquer” (Sharpe 1850); NW and NE parts of Arruda subbasin.

Type horizon: “Subcretaceous limestone” (Sharpe 1850); presumably Sobral member of the Farta Pao formation (Upper Kimmeridgian/Lower Tithonian).

Original diagnosis.—“Cordato-triangular, with the dorsal margin continued in a regular curve from the umbo to the posterior angle; ventral margin rounded; anterior margin with a deep depression below the beaks, which are placed very forward. The dorsal side is nearly perpendicular to the rest of the valve and marked with two slight longitudinal carinae. Surface nearly smooth, with some concentric wrinkles which are stronger near the ventral margin.” (Sharpe 1850).

Description.—Shell thick and rounded; slightly elongate to equally-sided sub-triangular in outline; slightly longer than high (average length/height ratio 1.2) and moderately inflated; relatively variable in shape; beaks moderately to strongly prosogyrous. Lunula medium-sized in young individuals, becoming relatively smaller in adulthood. Two distinct radial ridges descending from beak in posterior part of shell. First ridge slightly rounded, bordering main disc towards a small posterior band. Pronounced second ridge separating entire disc from markedly impressed acute-oval area, extending almost to ventral margin. Escutcheon deeply incised, stretching over almost half of the posterior dorsal shell margin. Disc ornamented with more or less distinct, slightly irregular commarginal growth lines. Commarginal lamellae prominent in young individuals at anterior shell portion, fading in central part of disc; reappearing at posterior part, running across first radial ridge up to summit of second ridge (Fig. 5E, G). Lamellae lacking in adulthood. Pallial line integripalliat. Adductor muscle scars relatively small, round-elliptic, almost equally sized. Hinge plate broad, triangular. Right valve: 3a relatively small, knob-like triangular, almost fused with hinge plate at lower end. 3b broad and prominent, elongated-triangular. 5b weakly developed, slender. AI broadened and more prominent in upper part, clearly separated from antero-dorsal shell margin by distinct furrow; distinctly set off from 3a. P1 sharp and prominent, distinctly elevated in lower part. Left valve: 2b well-developed. 4b elongated, distinct, almost fused with P2. A2 slender and distinct, clearly set off from 2b. Nymphs long and prominent, extending considerably above the escutcheon margin.

Remarks.—Although size increase in *Eomiodon securiformis* is obvious and stratigraphically younger specimens tend to display less elongated shell shapes, a separation of two stratigraphically and/or morphologically distinct species is impossible. From most other species, *E. securiformis* is easily distinguished by its much larger size. Probably most closely related to *E. securiformis* is *Eomiodon cuneatus* (Sowerby, 1816), occurring in Upper Jurassic strata of Great Britain, France, and northern Germany (de Loriol and Pellat 1866; de Loriol et al. 1872; Huckriede 1967). This species also displays a certain size increase during the Late Jurassic in northern Germany, which was, however, not recorded in detail, but seems to have occurred rather gradually (Huckriede 1967). However, even the “giant forms” mentioned by Huckriede (1967) hardly

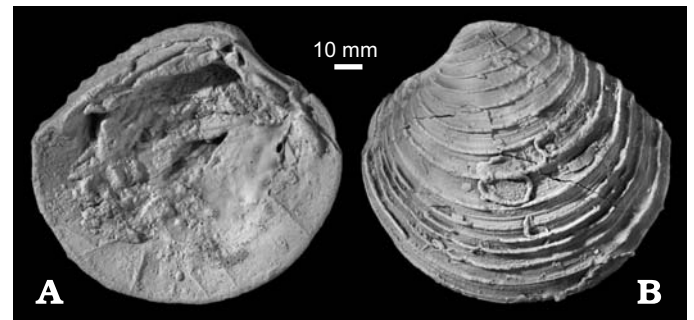


Fig. 16. Left valve of neomiodontid bivalve *Eomiodon* sp. from Early Tithonian, Arranhó II member, Santa Cruz (GML 25929) in internal (A) and external (B) views.

reach 45 mm in length, while *E. securiformis* frequently attains lengths of more than 60 mm, with a maximum size of 85 mm. Moreover, *E. cuneatus* is generally more triangular in outline, with a more elongated and pointed postero-ventral shell portion. Additionally, the radial ridges in the posterior shell part are less prominent. To date, *E. securiformis* has never been recorded from outside the Lusitanian Basin. The specimen figured by Contejean (1860) as “*Cyprina securiformis* Contej.” is an internal mold, and cannot be determined to genus or species; the presence of only one extremely sharp, radial ridge and the large posterior shell part, which is almost rectangular to the disc clearly indicate that this is not *E. securiformis*. However, a single, beautifully preserved articulated specimen from the Lower Kimmeridgian of the Algarve region, housed at the BSPG, is clearly *E. securiformis* and therefore prevents us from considering the species a form endemic to the Lusitanian Basin.

A second, previously undescribed species of *Eomiodon* (*Eomiodon* sp. A of Werner 1986) occurs in the Alcobaça and Farta Pao formations (Arranhó II member) (Fig. 16). These specimens hardly reach a length of 15 mm. However, it is obvious that they do not represent juvenile *E. securiformis*, as they are nearly circular in outline, while *E. securiformis* is markedly triangular even in early growth stages. Moreover, *Eomiodon* sp. A is ornamented with prominent regular commarginal lamellae, which are continuously well-developed from the anterior to the posterior margin, while the lamellae in young *E. securiformis* are more widely spaced and fade on the posterior flank just to reappear behind a weakly developed radial carina that is not present in *E. sp. A*. The escutcheon area in *E. securiformis* is much larger than in *E. sp. A*, and the nymph commonly rises above the inner shell margin. Additionally, the anterior lateral tooth (A2) in *E. sp. A* is much stronger developed than in *E. securiformis*.

Conclusions

As far as we are aware, the present study is the most extensive quantitative report on morphometric changes in Juras-

sic bivalves to date. The results provide valuable insights in the morphologic plasticity of bivalve shells and the development of taxa within a geographically confined area. The three genera studied show similar evolutionary patterns of morphologic development within the Upper Jurassic of the Lusitanian Basin, but all of them yield specific peculiarities. All target taxa display a distinct, sudden size increase shortly after the Early to Late Kimmeridgian transition, at approximately 152 million years before present. In contrast to the general, continuous gradual evolutionary size increase (Cope's Rule) documented for numerous bivalve groups during the Jurassic, this process occurs relatively rapid in our target taxa and must have been triggered by substantial environmental changes. A variety of potential reasons, such as changes in the rate of sedimentation, salinity, climate, or sea water chemistry, can widely be excluded. We hypothesise that size increase resulted from an increase in food supply due to enhanced phytoplankton productivity. Likely, nutrient input by freshwater runoff increased due to the progradation of continental facies in the Lusitanian Basin. However, size did not increase simultaneously in all genera. Data on *Eomiodon* do not permit to pinpoint this event precisely; in *Isognomon*, however, larger size is obviously achieved slightly earlier than in *Arcomytilus*. This pattern may suggest varied rates of adaptation in different bivalve taxa.

External ecological factors seem to have little or no control on shell shape in the target taxa. Generally, great variability is displayed rather within than between populations. In *Arcomytilus morrisii*, straight, blunt and stout shells point to a more or less epibyssate fixation, while incurved, triangular shells with tapering beaks indicate an endobyssate mode of life. Both shell types frequently occur within populations. However, the broad triangular type predominantly occurs in more fine-grained, muddy or argillaceous substrate of the Arranhó I [5] and Arranhó II [6] members. Likely, this shape change results from size increase and from adaptation to soft substrates prevailing in the favourite settings of *A. morrisii*, i.e., quiet, shallow lagoons with reduced salinity conditions. Additionally, greater exposition and consequently advantages in competition for food may have favoured the development of higher, more triangular shells. The number of ribs in *Arcomytilus* is largely independent of shape, but may be related to facies to a certain extent, as specimens with less numerous ribs preferentially occur in soft, soupy substrates.

A pattern similar to *Arcomytilus* is observed in *Isognomon*. Shell outline variability slightly increased with time, leading to the establishment of triangular shell shapes with more tapering umbones and higher ligamental areas, which, however, co-occur with specimens of "normal" shape. Any ecophenotypy could not be distinguished. Size increase in *Isognomon* co-occurs with a substantial change in the number of resilifers per ligament length, resulting in the development of a new species. The Late Oxfordian to Early Kimmeridgian *Isognomon rugosus* is characterised by a density of 3.3 resilifers per centimetre, while its descendent, the Late

Kimmeridgian to Early Tithonian *Isognomon lusitanicus* exhibits only 1.8 resilifers per centimetre.

Although the shells of *Eomiodon securiformis* are quite variable in outline, there is no indication of ecophenotypy. A trend towards higher, less elongated shapes, concurring with size increase may indicate an adaptation to lower burrowing depth and probably settlement in comparatively quiet lagoonal settings.

For all target genera, the Late Jurassic represents only a minor segment of their total temporal ranges (*Arcomytilus*: Lower Jurassic–Eocene, Soot-Ryen 1969; *Isognomon*: Upper Triassic–Recent, Cox 1969; *Eomiodon*: Lower Jurassic–Upper Cretaceous, Casey 1969). Consequently, the evolutionary pattern unravelled by this study may be further extrapolated to other areas and/or time slices, although the restricted environments of the semi-enclosed Lusitanian Basin may have led to the establishment of evolutionary mechanisms different from those acting in open marine settings.

Acknowledgements

The following persons are acknowledged for their contribution to this study: Miguel M. Ramalho (IGM) kindly provided access to the collection of León Paul Choffat at the GML. Octávio Mateus (Museu do Jurássico, Lourinhã, Portugal) is acknowledged for fruitful discussions and logistic support. Didier Merle and Hervé Senut (both MNHN) kindly provided access to the collections and facilities at the MNHN. Henning Scholz (Museum für Naturkunde, Berlin, Germany) provided literature and software. Gernot Arp (University of Göttingen, Göttingen, Germany) provided information on the Jurassic in Northern Germany. Christoph Mayr (Ludwig-Maximilians-University, Munich, Germany) performed the oxygen isotope analyses and provided literature. Georg Janßen (Ludwig-Maximilians-University, Munich, Germany) prepared the photographs. Franziska Maier, Ulrich Projahn, and Stefan Sónyi (all BSPG) carried out the extensive preparation work that was needed to provide nearly 1400 usable bivalve specimens. Christine Böhmer (BSPG) greatly helped with production of data sets. The study benefited considerably from the careful reviews by James Crampton (GNS Science, Lower Hutt, New Zealand), Michal Kowalewski (Virginia Tech, Blacksburg, USA), and Marcin Machalski (Institute of Paleobiology PAS, Warszawa, Poland). The project was funded by the Deutsche Forschungsgemeinschaft (projects Fu 131/31-2 and We 1152/2-2).

References

- Aguirre, M.L., Perez, S.I., and Sirch, Y.N. 2006. Morphological variability of *Brachidontes* Swainson (Bivalvia, Mytilidae) in the marine Quaternary of Argentina (SW Atlantic). *Palaeogeography, Palaeoclimatology, Palaeoecology* 239: 100–125. <http://dx.doi.org/10.1016/j.palaeo.2006.01.019>
- Akster, R.J. and Martel, A.L. 2000. Shell shape, dysodont tooth morphology, and hinge-ligament thickness in the bay mussel *Mytilus trossulus* correlate with wave exposure. *Canadian Journal of Zoology* 78: 240–253. <http://dx.doi.org/10.1139/cjz-78-2-240>
- Alves, T.M., Gawthorpe, R.L., Hunt, D.W., and Monteiro, J.H. 2002. Jurassic tectono-sedimentary evolution of the northern Lusitanian Basin (off-shore Portugal). *Marine and Petroleum Geology* 19: 727–754. [http://dx.doi.org/10.1016/S0264-8172\(02\)00036-3](http://dx.doi.org/10.1016/S0264-8172(02)00036-3)

- Alves, T.M., Manupella, G., Gawthorpe, R.L., Hunt, D.W., and Monteiro, J.H. 2003. The depositional evolution of diapir- and fault-bounded rift basins: examples from the Lusitanian Basin of West Iberia. *Sedimentary Geology* 162: 273–303. [http://dx.doi.org/10.1016/S0037-0738\(03\)00155-6](http://dx.doi.org/10.1016/S0037-0738(03)00155-6)
- Alves, T.M., Moita, C., Sandnes, F., Cunha, T., Monteiro, J.H., and Pinheiro, L.M. 2006. Mesozoic–Cenozoic evolution of North Atlantic continental-slope basins; the Peniche Basin, western Iberian margin. *American Association of Petroleum Geologists, Bulletin* 90: 31–60.
- Amler, M.R.W. 1999. Synoptical classification of fossil and recent Bivalvia. *Geologica et Palaeontologica* 33: 237–248.
- Anderson, L.C. and Roopnarine, P.D. 2005. Role of constraint and selection in the morphologic evolution of *Caryocorbula* (Mollusca: Corbulidae) from the Caribbean Neogene. *Palaeontologia Electronica* 8 (2): 1–18.
- Anderson, T.F. and Arthur, M.A. 1983. Stable isotopes of oxygen and carbon and their application to sedimentologic and environmental problems. *SEPM Short Courses Notes* 10: 1.1–1.151.
- Anderson, T.F., Popp, B.N., Williams, A.C., Ho, L.-Z., and Hudson, J.D. 1994. The stable isotopic records of fossils from the Peterborough Member, Oxford Clay Formation (Jurassic), UK: palaeoenvironmental implications. *Journal of the Geological Society, London* 151: 125–138. <http://dx.doi.org/10.1144/gsjgs.151.1.0125>
- Blakey, R.C. 2007. (December 04): *Detailed global paleogeography*. Available from: <http://jan.ucc.nau.edu/~rcb7/globaltext2.html>.
- Bond, J.E. and Beamer, D.A. 2006. A morphometric analysis of mygalomorph spider carapace shape and its efficacy as a phylogenetic character (Araneae). *Invertebrate Systematics* 20: 1–7. <http://dx.doi.org/10.1071/IS05041>
- Buffetaut, E., Bülow, M., Gheerbrant, E., Jaeger, J.-J., Martin, M., Mazin, J.-M., Milsent, C., and Rioult, M. 1985. Biostratigraphical zonation and new vertebrate remains in the “Sables de Glos” (Upper Oxfordian, Normandy). *Comptes Rendus de l’Académie des Sciences, Série II. Mécanique-Physique-Chimie-Sciences de l’univers-Sciences de la terre* 300: 929–932.
- Carvalho, J., Matias, H., Torres, L., Manuppella, G., Pereira, R., and Mendes-Victor, L. 2005. The structural and sedimentary evolution of the Arruda and Lower Tagus Sub-basins, Portugal. *Marine and Petroleum Geology* 22: 427–453. <http://dx.doi.org/10.1016/j.marpetgeo.2004.11.004>
- Casey, R. 1969. Family Neomiodontidae Casey, 1955. In: R.C. Moore (ed.), *Treatise on Invertebrate Paleontology, Part N, Mollusca 6, Bivalvia 2*, N653–N655. Kansas University Press, Lawrence.
- Chavan, C. 1952. Les Pélécy-podes des sables astartiens de Cordebugles (Calvados). *Schweizerische Palaeontologische Abhandlungen* 69: 1–132.
- Choffat, P. 1885. Description de la faune jurassique du Portugal. Mollusques Lamellibranches 2^e ordre. Asiphonida. *Mémoires de la Direction des Travaux Géologiques du Portugal* 1885: 1–76.
- Choffat, P. 1893. Description de la faune jurassique du Portugal. Mollusques Lamellibranches Premier ordre. Siphonida. *Mémoires de la Direction des Travaux Géologiques du Portugal* 1893: 1–39.
- Contejean, Ch. 1860 [for 1859]. Étude de l’étage Kimméridgien dans les environs de Montbéliard et dans le Jura. *Mémoires de la Société d’Emulation du Doubs* 1860: 1–352.
- Cox, L.R. 1969. Family Isognomonidae Woodring, 1925. In: R.C. Moore (ed.), *Treatise on Invertebrate Paleontology, Part N, Mollusca 6, Bivalvia 1*, N321–N326. Kansas University Press, Lawrence.
- Cox, L.R., Nuttall, C.P., and Trueman, E.R. 1969. General features of Bivalvia. In: R.C. Moore (ed.), *Treatise on Invertebrate Paleontology, Part N, Mollusca 6, Bivalvia 1*, N2–N129. Kansas University Press, Lawrence.
- Crampton, J.S. and Gale, A.S. 2005. A plastic boomerang: speciation and intraspecific evolution in the Cretaceous bivalve *Actinoceramus*. *Paleobiology* 31: 559–577.
- Crampton, J.S. and Gale, A.S. 2009. Taxonomy and biostratigraphy of the Late Albian *Actinoceramus sulcatus* lineage (Early Cretaceous Bivalvia, Inoceramidae). *Journal of Paleontology* 83: 89–109. <http://dx.doi.org/10.1666/08-037R.1>
- Crampton, J.S. and Haines, A.J. 1996. Users’ manual for programs Hangle, Hmatch and Hcurve for the Fourier shape analysis of two-dimensional outlines. *Institute of Geological and Nuclear Sciences, Science Report* 96: 1–28.
- Crampton, J.S. and Maxwell, P.A. 2000. Size: All it’s shaped up to be? Evolution of shape through the lifespan of the Cenozoic bivalve *Spissatella* (Crassatellidae). In: E.M. Harper, J.D. Taylor, and J.A. Crame (eds.), *The Evolutionary Biology of the Bivalvia*, 399–423. Geological Society, London.
- Delvene, G. 2007. Middle and Upper Jurassic bivalves from the Geomining Museum collections (IGME, Geological Survey of Spain). *Beringeria* 37: 11–31.
- Delvene, G. and Fürsich, F.T. 2002. Catálogo de los bivalvos españoles del Jurásico Medio y Superior depositados en el Museo Geominero (IGME, Madrid). *Boletín Geológico y Minero* 113: 199–210.
- Enay, R. 1997. Le Jurassique Supérieur. In: E. Cariou and P. Hantzpergue (eds.), *Biostratigraphie du Jurassique Ouest-Européen et Méditerranéen. Zonations parallèles et distribution des invertébrés et microfossiles. Bulletin des Centres de Recherches Exploration-Production Elf-Aquitaine, Mémoire* 17: 363–369.
- Epstein, S., Buchsbaum, R., Lowenstam, H.A., and Urey, H.C. 1951. Carbonate-water isotopic temperature scale. *Geological Society of America, Bulletin* 62: 417–426. [http://dx.doi.org/10.1130/0016-7606\(1951\)62%5B417:CITS%5D2.0.CO;2](http://dx.doi.org/10.1130/0016-7606(1951)62%5B417:CITS%5D2.0.CO;2)
- Freneix, S. and Quesne, H. 1985. Une espèce nouvelle du Kimméridgien du Portugal (Estremadura): *Aulacomyella abadiensis* nov. sp. (Bivalvia, Posidoniidae). *Geobios* 18: 371–376. [http://dx.doi.org/10.1016/S0016-6995\(85\)80099-1](http://dx.doi.org/10.1016/S0016-6995(85)80099-1)
- Fürsich, F.T. 1980. Preserved life positions of some Jurassic bivalves. *Paläontologische Zeitschrift* 54: 289–300.
- Fürsich, F.T. 1981a. Salinity-controlled benthic associations from the Upper Jurassic of Portugal. *Lethaia* 14: 203–223. <http://dx.doi.org/10.1111/j.1502-3931.1981.tb01690.x>
- Fürsich, F.T. 1981b. *Jurassicorbula* n. gen., a new bivalve genus from the Upper Jurassic of Portugal. *Neues Jahrbuch für Geologie und Paläontologie, Monatshefte* 1981: 737–741.
- Fürsich, F.T. 1994. Palaeoecology and evolution of Mesozoic salinity-controlled benthic macroinvertebrate associations. *Lethaia* 26: 327–346. <http://dx.doi.org/10.1111/j.1502-3931.1993.tb01540.x>
- Fürsich, F.T. and Aberhan, M. 1990. Significance of time-averaging for palaeocommunity analysis. *Lethaia* 23: 143–152.
- Fürsich, F.T. and Schmidt-Kittler, N. 1980. Biofacies analysis of Upper Jurassic marginally marine environments of Portugal. I. The carbonate-dominated facies at Cabo Espichel, Estremadura. (With a contribution of M. Ramalho). *Geologische Rundschau* 69: 943–981. <http://dx.doi.org/10.1007/BF02104654>
- Fürsich, F.T. and Werner, W. 1984. Salinity zonation of benthic associations in the Upper Jurassic of the Lusitanian Basin (Portugal). *Geobios, Mémoire spécial* 8: 85–92. [http://dx.doi.org/10.1016/S0016-6995\(84\)80160-6](http://dx.doi.org/10.1016/S0016-6995(84)80160-6)
- Fürsich, F.T. and Werner, W. 1985. New species of brackish water Bivalvia from the Upper Jurassic of Portugal. *Neues Jahrbuch für Geologie und Paläontologie, Monatshefte* 1985: 438–448.
- Fürsich, F.T. and Werner, W. 1986. Benthic associations and their environmental significance in the Lusitanian Basin (Upper Jurassic, Portugal). *Neues Jahrbuch für Geologie und Paläontologie, Abhandlungen* 172: 271–329.
- Fürsich, F.T. and Werner, W. 1988. The Upper Jurassic Bivalvia of Portugal. Part I. Palaeotaxodonta and Pteriomorphia (Arcoida and Mytiloida). *Comunicações dos Serviços Geológicos de Portugal* 73: 103–144.
- Fürsich, F.T. and Werner, W. 1989a. The Upper Jurassic Bivalvia of Portugal. Part II. Pteriomorphia (Pteroida exclusive Ostreina). *Comunicações dos Serviços Geológicos de Portugal* 74: 105–164.
- Fürsich, F.T. and Werner, W. 1989b. Taxonomy and ecology of *Juranomia calcibysata* gen. et sp. nov.—a widespread anomiid bivalve from the Upper Jurassic of Portugal. *Geobios* 22: 325–337. [http://dx.doi.org/10.1016/S0016-6995\(89\)80135-4](http://dx.doi.org/10.1016/S0016-6995(89)80135-4)

- Fürsich, F.T. and Werner, W. 1991. Palaeoecology of coralline sponge-coral meadows from the Upper Jurassic of Portugal. *Paläontologische Zeitschrift* 65: 35–69.
- Fürsich, F.T., Werner, W., and Schneider, S. 2009. Autochthonous to parautochthonous bivalve concentrations within transgressive marginal marine strata of the Upper Jurassic of Portugal. *Palaeobiodiversity and Palaeoenvironments* 89: 161–190.
- Gardner, J.P.A. 2004. A historical perspective of the genus *Mytilus* (Bivalvia: Mollusca) in New Zealand: multivariate morphometric analyses of fossil, midden and contemporary blue mussels. *Biological Journal of the Linnean Society* 82: 329–344. <http://dx.doi.org/10.1111/j.1095-8312.2004.00362.x>
- Gosling, E. 1992a. Systematics and geographic distribution of *Mytilus*. In: E. Gosling (ed.), *The mussel Mytilus: Ecology, physiology, genetics and culture*. *Developments in Aquaculture and Fisheries Science* 25: 1–20.
- Gosling, E. 1992b. Genetics of *Mytilus*. In: E. Gosling (ed.), *The mussel Mytilus: ecology, physiology, genetics, and culture*. *Developments in Aquaculture and Fisheries Science* 25: 309–382.
- Goldfuss, G.A. 1826–44. *Petrefacta Germaniae*. 692 pp. Arnz, Düsseldorf.
- Gould, G.C. and MacFadden, B.J. 2004. Gigantism, dwarfism, and Cope's Rule: "Nothing in evolution makes sense without a phylogeny". *American Museum of Natural History Bulletin* 285: 219–237. [http://dx.doi.org/10.1206/0003-0090\(2004\)285%3C0219:C%3E2.0.CO;2](http://dx.doi.org/10.1206/0003-0090(2004)285%3C0219:C%3E2.0.CO;2)
- Haines, A.J. and Crampton, J.S. 2000. Improvements to the method of Fourier shape analysis as applied in morphometric studies. *Palaeontology* 43: 765–783. <http://dx.doi.org/10.1111/1475-4983.00148>
- Hallam, A. 1968. Morphology, palaeoecology and evolution of the genus *Gryphaea* in the British Lias. *Philosophical Transactions of the Royal Society of London, Series B* 234: 91–128. <http://dx.doi.org/10.1098/rstb.1968.0014>
- Hallam, A. 1975. Evolutionary size increase and longevity in Jurassic bivalves and ammonites. *Nature* 258: 493–496. <http://dx.doi.org/10.1038/258493a0>
- Hallam, A. 1998. The determination of Jurassic environments using palaeoecological methods. *Bulletin de Societé géologique de France* 169: 681–687.
- Hajkr, O., Růžička, B., and Prantl, F. 1960. Biometrical study of the outline of some mytiloid pelecypods. *Sborník Národního Muzea v Praze* 17: 81–95.
- Hammer, Ø., Harper, D.A.T., and Ryan, P.D. 2001. PAST: Palaeontological Statistics software package for education and data analysis. *Palaeontologia Electronica* 4 (1): 1–9.
- Harzhauser, M. and Mandic, O. 2008. Neogene lake systems of Central and South-Eastern Europe: Faunal diversity, gradients and interrelations. *Palaeogeography, Palaeoclimatology, Palaeoecology* 260: 417–434. <http://dx.doi.org/10.1016/j.palaeo.2007.12.013>
- Huckriede, R. 1967. Molluskenfaunen mit limnischen und brackischen Elementen aus Jura, Serpultit und Wealden NW-Deutschlands und ihre paläogeographische Bedeutung. *Beihefte zum Geologischen Jahrbuch* 67: 1–263.
- Jackson, D.A. 1993. Stopping rules in principal components analysis: a comparison of heuristical and statistical approaches. *Ecology* 74: 2204–2214. <http://dx.doi.org/10.2307/1939574>
- Johnson, A.L.A. 1984. The palaeobiology of the bivalve families Pectinidae and Propeamussiidae in the Jurassic of Europe. *Zitteliana* 11: 1–235.
- Johnson, A.L.A. 1994. Evolution of European Lower Jurassic *Gryphaea* (*Gryphaea*) and contemporaneous bivalves. *Historical Biology* 7: 167–186. <http://dx.doi.org/10.1080/10292389409380451>
- Johnson, A.L.A. 1999. Evidence and cause of small size in Bathonian (Middle Jurassic) marine bivalves of north-western Europe. *Palaeontology* 42: 605–624. <http://dx.doi.org/10.1111/1475-4983.00088>
- Katz, M.E., Wright, J.D., Miller, K.G., Cramer, B.S., Fennel, K., and Falkowski, P.G. 2005. Biological overprint of the geological carbon cycle. *Marine Geology* 217: 323–338. <http://dx.doi.org/10.1016/j.margeo.2004.08.005>
- Kidwell, S.M. and Bosence, D.W.J. 1991. Taphonomy and time-averaging of marine shelly faunas. In: P.A. Allison and D.E.G. Briggs (eds.), *Taphonomy. Releasing the data locked in the fossil record*. *Topics in Geobiology* 9: 116–209.
- Kirby, M.X., Soniat, T.M., and Spero, H.J. 1998. Stable isotope sclerochronology of Pleistocene and Recent oyster shells (*Crassostrea virginica*). *Palaios* 13: 560–569. <http://dx.doi.org/10.2307/3515347>
- Kuhl, F.P. and Giardina, C.R. 1982. Elliptic Fourier features of a closed contour. *Computer graphics and image processing* 18: 236–258. [http://dx.doi.org/10.1016/0146-664X\(82\)90034-X](http://dx.doi.org/10.1016/0146-664X(82)90034-X)
- Lee, T. and Ó Foighil, D. 2004. Hidden Floridian biodiversity: mitochondrial and nuclear gene trees reveal four cryptic species within the scorched mussel, *Brachidontes exustus*, species complex. *Molecular Ecology* 13: 3527–3542. <http://dx.doi.org/10.1111/j.1365-294X.2004.02337.x>
- Lee, T. and Ó Foighil, D. 2005. Placing the Floridian marine genetic disjunction into a regional evolutionary context using the "scorched mussel" *Brachidontes exustus* species complex. *Evolution* 59: 2139–2358.
- Leinfelder, R.R. 1986. Facies, stratigraphy and paleogeographic analysis of Upper? Kimmeridgian to Upper Portlandian sediments in the environs of Arruda dos Vinhos, Estremadura, Portugal. *Münchener Geowissenschaftliche Abhandlungen A* 7: 1–215.
- Leinfelder, R.R. and Wilson, R.C.L. 1998. Third-order sequences in an upper Jurassic rift-related second-order sequence, central Lusitanian Basin, Portugal. *SEPM Special Publications* 60: 507–525.
- Lestrel, P.E. 1989. Method for analyzing complex two-dimensional forms: elliptical Fourier functions. *American Journal of Human Biology* 1: 149–164. <http://dx.doi.org/10.1002/ajhb.1310010204>
- Liow, L.H. 2006. Do deviants live longer? Morphology and longevity in trachyleberidid ostracodes. *Paleobiology* 32: 55–69.
- Loriol, P. de and Cotteau, G. 1868. Monographie paléontologique et géologique de l'étage portlandien du département de l'Yonne. *Bulletin de la Société des Sciences historiques et naturelles de l'Yonne* 1 (2): 1–260.
- Loriol, P. de and Pellat, E. 1866. Monographie paléontologique et géologique de l'étage Portlandien des environs de Boulogne-sur-Mer. *Mémoires de la Société de Physique et d'Histoire naturelle de Genève* 19 (1): 1–200.
- Loriol, P. de and Pellat, E. 1874–75. Monographie paléontologique et géologique des étages supérieurs de la formation jurassique des environs de Boulogne-sur-Mer. *Mémoires de la Société de Physique et d'Histoire naturelle de Genève* 23: 1–155 [1874], 157–326 [1875].
- Loriol, P. de, Royer, E., and Tombeck, H. 1872. Description géologique et paléontologique des étages jurassiques supérieurs de la Haute-Marne. *Mémoires de la Société Linnéenne de Normandie* 16: 1–542.
- Maas, P.A.Y., O'Mullan, G.D., Lutz, R.A., and Vrijenhoek, R.C. 1999. Genetic and morphometric characterization of mussels (Bivalvia: Mytilidae) from Mid-Atlantic hydrothermal vents. *Biological Bulletin* 196: 265–272. <http://dx.doi.org/10.2307/1542951>
- Martin, R.E., Quigg, A., and Podkovyrov, V. 2008. Marine biodiversification in response to evolving phytoplankton stoichiometry. *Palaeogeography, Palaeoclimatology, Palaeoecology* 258: 277–291. <http://dx.doi.org/10.1016/j.palaeo.2007.11.003>
- McArthur, J.M., Doyle, P., Leng, M.J., Reeve, K., Williams, C.T., Garcia-Sanchez, R., and Howarth, R.J. 2007a. Testing palaeo-environmental proxies in Jurassic belemnites: Mg/Ca, Sr/Ca, Na/Ca, $\delta^{18}\text{O}$ and $\delta^{13}\text{C}$. *Palaeogeography, Palaeoclimatology, Palaeoecology* 252: 464–480. <http://dx.doi.org/10.1016/j.palaeo.2007.05.006>
- McArthur, J.M., Janssen, N.M.M., Reboulet, S., Leng, M.J., Thirlwall, M.F., and van de Schootbrugge, B. 2007b. Palaeotemperatures, polar ice-volume, and isotope stratigraphy (Mg/Ca, $\delta^{18}\text{O}$, $\delta^{13}\text{C}$, $^{87}\text{Sr}/^{86}\text{Sr}$): The Early Cretaceous (Berriasian, Valanginian, Hauterivian). *Palaeogeography, Palaeoclimatology, Palaeoecology* 248: 391–430. <http://dx.doi.org/10.1016/j.palaeo.2006.12.015>
- Meléndez, G. and Atrops, F. 1999. Report of the Oxfordian–Kimmeridgian boundary working group. *International Subcommission on Jurassic Stratigraphy Newsletter* 26: 67–74.
- Mikkelsen, P.M. and Bieler, R. 2008. *Seashells of Southern Florida*. Living

- Marine Mollusks of the Florida Keys and Adjacent Regions. Bivalves.* 503 pp. Princeton University Press, Princeton.
- Montenat, C., Guery, F., and Jamet, M. 1988. Mesozoic evolution of the Lusitanian Basin; comparison with the adjacent margin. *Proceedings of the Ocean Drilling Program, Scientific Results* 103: 757–775.
- Moore, G.T., Hayashida, D.N., Ross, C.A. and Jacobson, S.R. 1992. Paleoclimate of the Kimmeridgian/Tithonian (Late Jurassic) world; I, Results using a general circulation model. *Palaeogeography, Palaeoclimatology, Palaeoecology* 93: 113–150.
[http://dx.doi.org/10.1016/0031-0182\(92\)90186-9](http://dx.doi.org/10.1016/0031-0182(92)90186-9)
- Müller, P., Geary, D.H., and Magyar, I. 1999. The endemic molluscs of the Late Miocene Lake Pannon: their origin, evolution, and family-level taxonomy. *Lethaia* 32: 47–60.
- Muster, H. 1995. Taxonomie und Paläobiogeographie der Bakevelliidae (Bivalvia). *Beringeria* 14: 3–161.
- Nori, L. and Lathuilière, B. 2003. Form and environment of *Gryphaea arcuata*. *Lethaia* 36: 83–96.
<http://dx.doi.org/10.1080/00241160310003081>
- Palmer, M., Pons, G.X., and Linde, M. 2004. Discriminating between geographical groups of a Mediterranean commercial clam (*Chamelea gallina* [L.]: Veneridae) by shape analysis. *Fisheries Research* 67: 93–98. <http://dx.doi.org/10.1016/j.fishres.2003.07.006>
- Perez Camacho, A., Labarta, U., and Beiras, R. 1995. Growth of mussels (*Mytilus edulis galloprovincialis*) on cultivation rafts: influence of seed source, cultivation site and phytoplankton availability. *Aquaculture* 138: 349–363. [http://dx.doi.org/10.1016/0044-8486\(95\)01139-0](http://dx.doi.org/10.1016/0044-8486(95)01139-0)
- Ponton, D. 2006. Is geometric morphometrics efficient for comparing otolith shape of different fish species? *Journal of Morphology* 267: 750–757. <http://dx.doi.org/10.1002/jmor.10439>
- Poppe, G.T. and Goto, Y. 1993. *European seashells. Volume 2. Scaphopoda, Bivalvia, Cephalopoda*. 221 pp. Christa Hemmen, Wiesbaden.
- Price, G.D. and Sellwood, B.W. 1994. Paleotemperatures indicated by Upper Jurassic (Kimmeridgian–Tithonian) fossils from Mallorca determined by oxygen isotope composition. *Palaeogeography, Palaeoclimatology, Palaeoecology* 110: 1–10.
[http://dx.doi.org/10.1016/0031-0182\(94\)90106-6](http://dx.doi.org/10.1016/0031-0182(94)90106-6)
- Printrakoon, C. and Tëmkin, I. 2008. Comparative ecology of two parapatric populations of *Isognomon* (Bivalvia: Isognomonidae) of Kungkraabaen Bay, Thailand. *The Raffles Bulletin of Zoology* (Supplement) 18: 75–94.
- Ramalho, M.M. 1971. Contribution à l'étude micropaléontologique et stratigraphique du Jurassique supérieur et du Crétacé inférieur des environs de Lisbonne (Portugal). *Memórias dos Serviços Geológicos de Portugal, nova série* 19: 1–212.
- Rasmussen, E.S., Lomholt, S., Andersen, C., and Vejbaek, O.V. 1998. Aspects of the structural evolution of the Lusitanian Basin in Portugal and the shelf and slope area offshore Portugal. *Tectonophysics* 300: 199–225.
[http://dx.doi.org/10.1016/S0040-1951\(98\)00241-8](http://dx.doi.org/10.1016/S0040-1951(98)00241-8)
- Renaud, S. and Michaux, J. 2004. Parallel evolution in molar outline of murine rodents: the case of the extinct *Malpaisomys insularis* (Eastern Canary Islands). *Zoological Journal of the Linnean Society* 142: 555–572.
<http://dx.doi.org/10.1111/j.1096-3642.2004.00140.x>
- Rohlf, J. 2008. *tpsDIG 2.12*. Available from: <http://life.bio.sunysb.edu/morph>.
- Roopnarine, P.D., Signorelli, J., and Laumer, C. 2008. Systematic, biogeographic and microhabitat-based morphometric variation of the bivalve *Anomalocardia squamosa* (Bivalvia: Veneridae, Chioninae) in Thailand. *The Raffles Bulletin of Zoology* (Supplement) 18: 95–102.
- Roopnarine, P.D. and Vermeij, G.J. 2000. One species becomes two: The case of *Chione cancellata*, the resurrected *C. elevata* and a phylogenetic analysis of *Chione*. *Journal of Molluscan Studies* 66: 517–534.
<http://dx.doi.org/10.1093/mollus/66.4.517>
- Rufino, M.M., Gaspar, M.B., Pereira, A.M., and Vasconcelos, P. 2006. Use of shape to distinguish *Chamelea gallina* and *Chamelea striatula* (Bivalvia: Veneridae): Linear and geometric morphometric methods. *Journal of Morphology* 267: 1433–1440.
<http://dx.doi.org/10.1002/jmor.10489>
- Savazzi, E. 1995. Parasite-induced teratologies in the Pliocene bivalve *Isognomon maxillatus*. *Palaeogeography, Palaeoclimatology, Palaeoecology* 116: 131–139. [http://dx.doi.org/10.1016/0031-0182\(94\)00097-R](http://dx.doi.org/10.1016/0031-0182(94)00097-R)
- Schneider, S. and Werner, W. 2007. Colour pattern preservation in *Fuersichella* n. gen. (Gastropoda: Neritopsoidae), bivalves, and echinid spines from the Upper Jurassic of Portugal. *Beringeria* 37: 143–160.
- Schneider, S., Fürsich, F.T., and Werner, W. 2009. Sr-isotope stratigraphy of the Upper Jurassic of central Portugal (Lusitanian Basin) based on oyster shells. *International Journal of Earth Sciences* 98: 1949–1970.
<http://dx.doi.org/10.1007/s00531-008-0359-3>
- Scholz, H. 2003. Taxonomy, ecology, ecomorphology, and morphodynamics of the Unionoida (Bivalvia) of Lake Malawi (East-Africa). *Beringeria* 33: 1–86.
- Scholz, H. and Hartman, J.H. 2007a. Paleoenvironmental reconstruction of the Upper Cretaceous Hell Creek Formation of the Williston Basin, Montana, USA: Implications from the quantitative analysis of unionid bivalve taxonomic diversity and morphologic disparity. *Palaios* 22: 24–34. <http://dx.doi.org/10.2110/palo.2005.p05-059r>
- Scholz, H. and Hartman, J.H. 2007b. Fourier analysis and the extinction of unionid bivalves near the Cretaceous–Tertiary boundary of the Western Interior, USA: Pattern, causes, and ecological significance. *Palaeogeography, Palaeoclimatology, Palaeoecology* 255: 48–63.
<http://dx.doi.org/10.1016/j.palaeo.2007.02.040>
- Schulz-Mirbach, T. and Reichenbacher, B. 2008. Fossil *Aphanius* (Teleostei, Cyprinodontiformes) from southwestern Anatolia (Turkey): A contribution to the evolutionary history of a hotspot of freshwater biodiversity. *Geodiversitas* 30: 5–20.
- Seilacher, A. 1984. Constructional morphology of bivalves: evolutionary pathways in primary versus secondary soft-bottom dwellers. *Palaeontology* 27: 207–237.
- Sellwood, B.W. and Valdes, P.J. 2006. Mesozoic climates: General circulation models and the rock record. *Sedimentary Geology* 190: 269–287.
<http://dx.doi.org/10.1016/j.sedgeo.2006.05.013>
- Sharp, Z. 2007. *Principles of Stable Isotope Geochemistry*. 344 pp. Pearson Education, Upper Saddle River, NY.
- Sharpe, D. 1850. On the Secondary district of Portugal which lies on the North of the Tagus. *Quarterly Journal of the Geological Society, London* 6: 135–201. <http://dx.doi.org/10.1144/GSL.JGS.1850.006.01-02.18>
- Smith, A.G., Smith, D., and Funnell, B.M. 1994. *Atlas of Mesozoic and Cenozoic Coastlines*. 99 pp. Cambridge University Press, Cambridge.
- Soot-Ryen, T. 1969. Superfamily Mytilacea Rafinesque, 1815. In: R.C. Moore (ed.), *Treatise on Invertebrate Paleontology, Part N, Mollusca* 6, Bivalvia 1, N271–N281. Kansas University Press, Lawrence.
- Sowerby, J. 1812–22. *The Mineral Conchology of Great Britain*. 383 pls. Meredith, London.
- Sowerby, J. 1842. *James Sowerby's Mineral-Conchologie Grossbritanniens oder ausgemalte Abbildungen und Beschreibungen der Schalthier-Überreste, welche zu verschiedenen Zeiten und in verschiedenen Tiefen der Erde erhalten worden sind*. German translation by E. Desor. With annotations and rectifications by L. Agassiz. 689 pp. Jent and Gassmann, Solothurn.
- SPSS INC. 2007. *SPSS Base 16.0 User's Guide*. 527 pp. SPSS Inc., Chicago.
- Stanley, S.M. 1970. Relation of shell form to life habits in the Bivalvia (Mollusca). *Geological Society of America, Memoir* 125: 1–296.
- Stanley, S.M. 1972. Functional morphology and evolution of byssally attached bivalve mollusks. *Journal of Paleontology* 46: 165–212.
- Stanley, S.M. 1979. *Macroevolution. Pattern and Process*. 332 pp. Freeman, San Francisco.
- Surge, D.M., Lohmann, K.C., and Dettman, D.L. 2001. Controls on isotopic chemistry of the American oyster, *Crassostrea virginica*: implications for growth patterns. *Palaeogeography, Palaeoclimatology, Palaeoecology* 172: 283–296.
- Surge, D.M., Lohmann, K.C., and Goodfriend, G.A. 2003. Reconstructing estuarine conditions: oyster shells as recorders of environmental change, southwest Florida. *Estuarine, Coastal and Shelf Science* 57: 737–756.
[http://dx.doi.org/10.1016/S0031-0182\(01\)00303-0](http://dx.doi.org/10.1016/S0031-0182(01)00303-0)
- Tang, C. and Pantel, J.H. 2005. Combining morphometric and paleoecological

- analyses: Examining small-scale dynamics in species-level and community-level evolution. *Palaeontologia Electronica* 8 (2): 1–10.
- Tebble, N. 1966. *British Bivalve Seashells*. 212 pp. HMSO, Edinburgh.
- Tëmkin, I. 2006. Morphological perspective on the classification and evolution of Recent Pterioidea (Mollusca: Bivalvia). *Zoological Journal of the Linnean Society* 148: 253–312.
<http://dx.doi.org/10.1111/j.1096-3642.2006.00257.x>
- Valdes, P.J. and Sellwood, B.W. 1992. A palaeoclimate model for the Kimmeridgian. *Palaeogeography, Palaeoclimatology, Palaeoecology* 95: 47–72. [http://dx.doi.org/10.1016/0031-0182\(92\)90165-2](http://dx.doi.org/10.1016/0031-0182(92)90165-2)
- Vermeij, G.J. 1990. Tropical Pacific pelecypods and productivity: a hypothesis. *Bulletin of Marine Science* 47: 62–67.
- Walker, K.R. and Bambach, R.K. 1971. The significance of fossil assemblages from fine-grained sediments: time-averaged communities. *Geological Society of America, Abstracts with Programs* 3: 783–784.
- Werner, W. 1986. Palökologische und biofazielle Analyse des Kimmeridge (Oberjura) von Consolação, Mittelportugal. *Zitteliana* 13: 3–109.
- Wierzbowski, H. 2002. Detailed oxygen and carbon isotope stratigraphy of the Oxfordian in Central Poland. *International Journal of Earth Sciences* 91: 304–314. <http://dx.doi.org/10.1007/s005310100217>
- Wierzbowski, H. and Joachimski, M. 2007. Reconstruction of late Bajocian–Bathonian marine palaeoenvironments using carbon and oxygen isotope ratios of calcareous fossils from the Polish Jura Chain (central Poland). *Palaeogeography, Palaeoclimatology, Palaeoecology* 254: 523–540. <http://dx.doi.org/10.1016/j.palaeo.2007.07.010>
- Willmann, R. 1985. *Die Art in Raum und Zeit. Das Artkonzept in der Biologie und Paläontologie*. 207 pp. Paul Parey, Berlin.
- Wilson, R.C.L. 1975. Atlantic opening and Mesozoic continental margin basins of Iberia. *Earth and Planetary Science Letters* 25: 33–43. [http://dx.doi.org/10.1016/0012-821X\(75\)90207-1](http://dx.doi.org/10.1016/0012-821X(75)90207-1)
- Wilson, R.C.L., Hiscott, R.N., Willis, M.G., and Gradstein, F.M. 1989. The Lusitanian Basin of west central Portugal: Mesozoic and Tertiary tectonic, stratigraphy and subsidence history. *American Association of Petroleum Geologists, Memoir* 46: 341–361.